THE UNIVERSITY OF ALBERTA

OPTICAL MODEL ANALYSIS OF P+⁴He ELASTIC SCATTERING

by

© STEPHEN WAI-LUEN LEUNG

A THESIS

SUBMITTED TO THE FACULTY OF GRADUATE STUDIES AND RESEARCH

IN PARTIAL FULFILMENT OF THE REQUIREMENTS FOR THE DEGREE

OF MASTER OF SCIENCE

IN

NUCLEAR PHYSICS

DEPARTMENT OF PHYSICS

EDMONTON, ALBERTA

SPRING, 1978

THE UNIVERSITY OF ALBERTA

FACULTY OF GRADUATE STUDIES AND RESEARCH

The undersigned certify that they have read, and recommend to the Faculty of Graduate Studies and Research, for acceptance, a thesis entitled OPTICAL MODEL ANALYSIS OF ... P.t. ^{4}He ELASTIC SCATTERING .....

.....

submitted by Stephen Wai-Luen Leung .....

in partial fulfilment of the requirements for the degree of Master of Science.

.....Henry S. Sherif...
Supervisor

...Richard B. Smyth...

...D. G. Hughes...

.....Anbarasu.....

DATE...Dec. 6, 1977....

To

My Family

ABSTRACT

The conventional Optical Potential Model has been used to analyze the P+⁴He elastic scattering data in the medium energy range (100 MeV ≤ Ep ≤ 1100 MeV). The model is successful in describing the data in this energy range. We find the complex spin-orbit potential plays an important role in obtaining a good fit to the data. An exchange potential is also found necessary for the reproduction of the large angle data.

The behaviour of the volume integral of the real central potential indicates a logarithmic energy dependence. A linear downward trend is observed as the proton energy increases and the Jr/A = 0 point occurs at about 450 MeV. The volume integral of the imaginary potential shows a general upward behaviour with increasing incident proton energy. The r.m.s. radius obtained agrees well with results obtained from other sources.

ACKNOWLEDGEMENTS

I would like to thank my supervisor Dr. Sherif who not only suggested this thesis but also helped in every possible way through out the course of this work.

Special thanks are due to Dr. Cameron for his involvement in the early stage of this work. Bob McCamies for providing a list of referencs and explanation on the computer code "SEEK".

The 'gentle' introduction to the experimental technique by Dr. Green, Dr. Lam, Dr. Yu and Dr. Fielding are very much appreciated. Thanks to Dr. Neilsen and Uncle Jock as they always available at momments of desperation.

I would like to thank all the technical and secretarial staff; Greta, Beth, Marlene, Lars, Little JOHN, Earl..... who provided a fond memory of the Nuclear Research Center.

Special thanks are due to Pasos, J. Easton and Uncle Ken for sharing their ' computer minds '.

I would like to thank my fellow comrades who through the long dark hours (night shifts) have taught me the necessites in becoming a Physics Student. Tom the Neutron, Rick Hooper, Ron Sloboda, Gordon Semenoff , Dave Henty, Larry Antonuk and Barb Paulson they have taught me so much especially the " Multiple Scattering Theory ".

And my most sincere thanks to my office mate Mr. Tim Cooper who not only show me the Glauber Theory and helped to put the thesis into present English form, but also show me

what a English really is !!

Finally, I would like to express my gratitude to my family for things too numerous to mention.

TABLE OF CONTENTS

CHAPTER	PAGE
1. Introduction	1
2. Theory	8
Introduction	8
Theory of the Optical Model Potential	9
3. Method of Analysis	20
Optical Potential Model	20
Data	21
Relativistic Corrections	22
Search Procedure	23
4. Results	28
5. Discussion and Concluson	50
Comparison	50
R.M.S. Radii and Volume Integrals.	56
Conclusion	61
References	68
Appendix. 'SEEK'	73

LIST OF TABLES

Table	Description	Page
1.	Data selection for the P+He⁴ Optical Model Analysis in the energy range of 100 Mev to 1150 Mev	27
2.	Optical Model Geometry	48
3.	Optical Model Parameters	49
4.	Optical Model Parameters from other referencs	67

LIST OF FIGURES

Figure		Page
1.	Optical Model fit to 100 MeV cross-section data	32
2.	Optical Model fit to 156 Mev cross-section data	33
3.	OPtical Model fit to 147 Mev polarization data at 156 Mev	34
4.	Optical Model fit to 203 MeV cross-section and polarization data	35
5.	Optical Model fit to 312 MeV cross-section and polarization data	36
6.	Optical Model fit to 350 MeV cross-section data	37
7.	Optical Model fit to 560 Mev cross-section and polarization data	38
8.	Optical Model fit to 560 MeV polarization data	39
9.	Optical Model fit to 650 MeV cross-secion data	40
10.	Optical Model fit to 720 meV cross-section data	41
11.	Optical Model fit to 720 MeV polarization data	42
12.	Optical Model fit to 800 MeV cross-section data	43
13.	Optical Model fit to 800 MeV polarization data	44
14.	Optical Model fit to 1030 MeV cross-section data	45
15.	Optical Model fit to 1030 MeV polarization data	46
16.	Optical model fit to 1150 MeV cross-section data	47
17.	Diagram illustrating r.m.s. distribution with energy	63
18.	Diagram illustrating Jr/A (the vol. integral) against Ep.	64
19.	Diagram illustrating Ji/A (Imaginary vol. integral) against Ep.	65

20. Diagram illustrating the effects of the exchange potential 66

CHAPTER 1

INTRODUCTION

It has long been understood that to study the interior of an atomic nucleus, the wave length of the projectile must be comparable to or shorter than the inter-nucleon spacing of the target nucleus. Therefore, probing the nucleus with high energy protons should be more fruitful for nuclear structure research than analogous experiments at lower energies.

Recently a large amount of effort has been devoted to the study of light nuclei with high energy protons. The pioneering work in this regard was that by Palevsky et al. (PA67), who obtained some interesting results for P+⁴He elastic scattering at 1 GeV. The differential cross-section was found to exhibit a sharp diffraction minimum. Since then, much experimental effort has been devoted to studing the P+⁴He system in the intermediate energy range (100 MeV ≤ Ep ≤ 1000 MeV) (PA67, GO70, CO75, GO68, VZ75, BE76, MC64, BO72, SC74, KL77) and a large amount of data were reported. The most interesting features observed about these data are the diffraction minimum at about $t = -.25 (GeV/c)^2$ (t is the square of the relativistic four - momentum transfer) for Ep ≥ 400 MeV and the rising back-angle cross-section for proton energies below 300 MeV and above 600 MeV.

The theoretical analysis of the data at medium energies was performed exclusively using either the Glauber

Approximation (GL59) or Optical Potential Model (WA57, KE59).

The Glauber Approximation, as developed by Glauber, assumes that :

1.) The target nucleons are stationary whilst the projectile passes through the target nucleus.

2.) Each collision between the incident projectile and a target nucleon is identical to the collision between free nucleons.

3.) The total change in phase of the particle wave function is equal to the sum of the phase changes which occur at each collision with a target nucleon.

4.) The Eikonal Approximation is also assumed to be valid.

The scattering amplitude $F(\Theta)$ for a spin-0 target is given by :

$$F(\Theta) = ik\int J_0(qb)(1 - \exp(i\chi(\vec{b}))) \, bdb \qquad 1.1$$

where $\vec{k}$ is the wave vector in the center of mass system, $\vec{q}$ is the momentum transfer, $\vec{b}$ is the impact parameter and $\chi(\vec{b})$ is the sum of the phases resulting from scattering with individual nucleons

$$\chi(\vec{b}) = \sum_j \chi_j (\vec{b}-\vec{s}_j) \qquad 1.2$$

where $\vec{s}$ represents the component of the target nucleon coordinate which is perpendicular to the propagation

direction $\vec{k}$.

The Glauber Approximation employed for the early analyses by Franco (FR65), Bessel and Wilkin (BE67, 68) , and Czyz and Lesniak (CZ67, 68, 70) was able to reproduce the dominant features of the data, but failed to explain the diffraction minimum. Frosch et al. (FR67) pointed out that the nuclear form factor should have a zero at about 10 fm^{-2} due to the result of their analysis. Hence, the gaussian form factor employed in the early analyses is inadequate for the ^4He nucleus.

The Optical Model Theory at high energies was first derived rigorously by Watson and collaborators (WA51, 53, 57) in a series of papers on multiple scattering at high energy. The basic assumption of the theory requires the Impulse Approximation to be valid, which allows a complicated many-body problem to be treated as many two-body problems. He related the multiple scattering to the Optical Model considering only on-shell elastic scattering for a large number of nucleons. A briefer derivation of Watson's Model is given in Chapter 2. Kerman et al. (K.M.T.) (KE59) took a slightly different approach, starting from the transition operator T, operating on the initial wave function $| 0, \vec{K} >$, where $| 0 >$ is the target ground state wave function. For a properly antisymmetrized state of the target nucleus

$$T = Av(1 + GT) \qquad 1.3$$

where A is the mass number, v is the two-body interaction potential and G is the 'Green Function. They defined an effective two-body interaction operator τ as:

$$\tau = v + vG\tau \qquad 1.4$$

to obtain the matrix element for a single particle projectile:

$$(A - 1)\langle 0,\vec{K}'|\tau|0,\vec{K}''\rangle \qquad 1.5$$

for states $\vec{K}'$ and $\vec{K}''$ of the incident particle.

The Optical Potential Model formulated by K.M.T. was used by Kujawski (KU70) and Feshbach et al. (Fe70, 71, 73) They included both the first and the second terms of the series in their analyses, where the second term of the series should be more sensitive to the nuclear structure. They were able to obtain reasonably good fits by including both spin and iso-spin effects.

Recently the Glauber Model regained some popularity due to the work by Wallace (WA71, 77). He expanded the amplitude in powers of the difference between the exact and eikonal propagators. He obtained a series having the Glauber Eikonal Approximation as the first term and which converges rapidly to the exact amplitude. The so called 'Wallace Corrections' were included in the analysis of the 1 GeV polarization and cross-section data by Wallace (WA77) and by Auger et al. (AU76) to analyze the data at 0.6, 0.72, 1.15 and 24 GeV. These authors obtained excellent fits to

the data by including both spin and iso-spin effects in their analyses.

The Optical Model and the Glauber Approximation can be related to each other by means of the Bessel transform. The idea was pursued by Dymarz et al. (DY77) who performed a phase shift calculation where the Glauber profile function was used to generate an optical potential. These authors were able to obtain good fits to the data. They compared their approach with the conventional Glauber Model approach and found the latter produced too deep a minimum.

Rule et al. (RU75a, 75b, 75c, 76) made an Effective Channel analysis of the P^{+}+He elastic scattering data. The elastic scattering of high energy particles by composite target nuclei is formulated in terms of coupled equations. The effects of inelastic processes are represented by an average inelastic channel. The theory incorporates approximately the effects of non-locality, energy dependence, rescattering and absorption due to all the inelastic channels. Although they ignored the spin-dependent effects, fair agreement was still obtained for the cross-section data at 0.59, 0.72, and 1.0 GeV

Phenomenological Optical Model analyses were performed by Clark et al. (AR75, 77). Using the Klein-Gordon Equation or the Dirac Equation, they employed a simple optical potential containing only a real and imaginary central potential as the fourth component of a potential four vector. Even though the spin-orbit potential was

ignored, good fits to the data were obtained.

In the lower energy region (Ep ≤ 400 MeV) most analyses were done by using either the conventional Optical Model with the Schrodinger Equation or the One Channel Resonating Group Theory. The method of resonating group structure has only been used to calculate cross-sections for scattering systems involving light nuclei. It essentially consists of building a completely antisymmetrized wave function for the whole system (target and projectile) from channel functions which correspond to the various ways of grouping the nucleons. This method is a microscopic approach which investigates the close interaction within the nucleus between these groups as opposed to looking at the nucleus as an average potential. For Ep around 100 MeV, it is necessary to introduce a phenomenological imaginary potential to account for all inelastic effects, therefore the beauty of a purely microscopic approach is lost. In general, the fits obtained by the Resonating Group Theory (RA74) and by the Optical Potential Model are equal in quality. However, the Optical Potential Model is more convenient for analyses in the same energy range.

The question of the significance of the spin-orbit potential has been raised in many of the analyses mentioned above. Clark et al. (AR76) have analyzed the data at a number of energies above 500 MeV. There has, as yet, been no attempt to perform an energy dependent analysis of all the experimental data from 100 to 1000 MeV. In this thesis we

want to examine the validity of using a conventional Optical Potential Model to fit the P+⁴He elastic scattering data and the effects of the spin-orbit potential in the medium energy range.

In chapter 2, we give a brief derivation of Watson's multiple scattering model and some of its characteristics. In chapter 3, we present a complete description of the method of analysis. In chapter 4, we compare the experimental data with our results at each corresponding energy. In chapter 5, we discuss our results as compared to other methods of analysis. The computing program 'SEEK' is described in Appendix 1.

CHAPTER 2

THEORY

2.1 Introduction

The Optical Potential Model has been used extensively to analyze elastic scattering experiments and direct reaction experiments. The theory is successful in describing both high and low energy nuclear experiments. The construction of the model is purely phenomenological and based on the assumption that the atomic nucleus can be treated as one single potential instead of a many-body interaction between the incident particle and the target nucleons. The question about the physical meaning of such a phenomenological model has been asked. Such a profound question has been answered by Watson and collaborators who provided the theoretical justification for the use of the Optical Model. In a series of papers on the theory of multiple scattering, Watson and his collaborators indicated the manner in which the Optical Potential for high energy nucleon-nucleus scattering could be calculated presupposing a knowledge of nucleon-nucleon interactions. Since we are only interested in elastic scattering, we shall give a simple derivation of the Optical Model for high energy elastic scattering. The derivation follows closely the work by Watson et al. (WA51, 57) and by Jones (JO63).

2.2 Theory of the Optical Model Potential

Let H_t be the Hamiltonian of the target nucleus, and e_n be the energy eigenvalue. The equation of motion for the nucleus is :

$$H_t|\xi\rangle = e_n|\xi\rangle \quad . \qquad 2.1$$

The target Hamiltonian is assumed to be hermitian and the states $|\xi\rangle$ are completely antisymmetric and form a complete orthogonal set with ground state $|\xi_0\rangle$. The equation of motion for the incident particle, when there is no interaction with the nucleus, is

$$H_p|\vec{k}'\rangle = E_p|\vec{k}'\rangle \qquad 2.2$$

where H_p is the free projectile Hamiltonian, E_p is the kinetic energy and $\vec{k}'$ is the momentum of the incident particle.

The first essential approximation is to neglect any antisymmetrization between the incident nucleon and the target nucleons. If there is no antisymmetrization with the incident particle, one can assume that the origin of the Optical Model Potential should coincide with the center of mass of the target nucleus for any mass number A. This assumption is common to all phenomenological Optical Model analyses. However, if the incident nucleon is antisymmetrized with the target nucleons, it is reasonable

to require that all A+1 nucleons should have a common single-particle potential with a specified origin. This condition does not seem to be possible due to the recoil of the target nucleons. Watson et al. (WA57) investigated the effects of antisymmetrization and found those effects to be small and unimportant.

The Schrodinger Equation we have to solve is :

$$(H_o + V)|\Psi\rangle = E|\Psi\rangle \qquad 2.3$$

where $H_o = H_t + H_p$

$E = e_n + E_p$

V is the interaction potential between the projectile and the target, and $|\Psi\rangle = |\xi, \vec{k}'\rangle$. Because both $|\xi\rangle$ and $|\vec{k}'\rangle$ are complete sets their product states $|\Psi\rangle$ must be both complete and orthogonal. The equivalent form of $|\Psi\rangle$ is :

$$|\Psi\rangle = |\xi_o, \vec{k}'\rangle + G(E)V|\Psi\rangle \qquad 2.4a$$

where

$$G(E) = (E - H_o + i\varepsilon)^{-1} \qquad 2.4b$$

The second term in (2.4a) includes the boundary condition of out-going scattered waves only, and $|\xi_o, \vec{k}'\rangle$ is the initial state wave function, consisting of a plane wave and the

ground state of the target nucleus.

The transition probability of the system depends on the matrix element of T, which is given by:

$$T = \langle \xi_0, \vec{k}' | V | \Psi \rangle \quad . \qquad 2.5$$

For elastic scattering, we can separate the ground state component by a projection operator β such that,

$$|\Phi\rangle = \frac{1}{(2\pi)^3} \int d\vec{k}'' |\xi_0, \vec{k}''\rangle\langle\xi_0, \vec{k}''|\Psi\rangle$$

$$= \beta|\Psi\rangle \qquad 2.6$$

The Optical Model operator is the interaction operator which leads to the elastic scattering state vector $|\Phi\rangle$ only. The Optical Model Operator is defined by the equation

$$|\Phi\rangle = |\xi_0, \vec{k}'\rangle + G(E)U|\Phi\rangle \quad . \qquad 2.7$$

The operator U must be such that it is incapable of changing the target ground state wave function into other excited states. Therefore we can write

$$\langle \xi, \vec{k}|U|\xi_0, \vec{k}'\rangle = \delta_{\xi\,\xi_0}\langle \vec{k}|U|\vec{k}'\rangle \qquad 2.8$$

and U is referred to as a single particle operator.

Following the derivation by Watson, we define an operator F such that

$$|\Psi\rangle = F|\Phi\rangle \qquad 2.9$$

Then

$$F = 1 + \tilde{G}(E)(V-U)F \qquad 2.10$$

where

$$\tilde{G}(E) = (E - U - H_0 + i\varepsilon)^{-1} \qquad 2.11$$

From (2.5), the elastic scattering amplitude can be written as

$$\langle \xi_0, \vec{k}' | U | \Phi \rangle = \langle \xi_0, \vec{k}' | V | \Psi \rangle \qquad 2.12$$

$$= \langle \xi_0, \vec{k}' | VF | \Phi \rangle \qquad 2.13$$

Substituting for F from (2.10), we have

$$\langle \xi_0, \vec{k}' | V[1+\tilde{G}(V-U)+\tilde{G}(V-U)\tilde{G}(V-U)+ \cdots] | \Phi \rangle \qquad 2.14$$

From the equation of $\tilde{G}(E)$, (2.4b) can be written as :

$$G(E) = [\, \tilde{G}^{-1}(E) + U \,]^{-1} \qquad 2.15$$

Using matrix algebra one can rewrite (2.15) as

$$G = \tilde{G} - \tilde{G}U\tilde{G} + \tilde{G}U\tilde{G}U\tilde{G} - \cdots \qquad 2.16$$

or

$$1 - GU = 1 - \tilde{G}U + \tilde{G}U\tilde{G}U - \tilde{G}U\tilde{G}U\tilde{G}U + \cdots . \qquad 2.17$$

Now, rearrange the series (2.14) as follows :

$$V(\tilde{G} - \tilde{G}U\tilde{G} + \cdots)V \cdots$$
$$\cdots (\tilde{G} - \tilde{G}U\tilde{G} + \cdots)V(1 - \tilde{G}U + \cdots). \qquad 2.18$$

Using (2.17) and (2.18) we can rewrite (2.14) as

$$\langle U \rangle = \langle (V + VGV + \cdots)(1 - GU) \rangle . \qquad 2.19$$

The intermediate states which may occur in the scattering process are such that either the incident particle or the target, or both, may be in excited states. It is convenient to separate the states in which only the incident nucleon is excited, with the target remaining in the ground state. This can be done by a projection operator defined by:

$$\alpha = 1 - \frac{1}{(2\pi)^3} \int d\vec{k}'' |\xi_0, \vec{k}''\rangle\langle\xi_0, \vec{k}''| \qquad 2.20a$$

and is related to β by:

$$1 = \alpha + \beta \qquad 2.20b$$

Now, the equation (2.14) can be written as:

$$\langle U \rangle = \langle | Y [\ 1 - G(\alpha+\beta)U\ ] | \rangle \qquad 2.21$$

$$= \langle | Y [\ 1 - \beta G U\ ] | \rangle$$

Recall that U only acts on the target ground state and a direct iteration of (2.21) gives

$$\langle U \rangle = \langle |\ Y - Y\beta G Y + Y\beta G Y \beta G Y + \cdots | \rangle \qquad 2.22$$

where

$$Y = V + VGV + \cdots \qquad 2.23$$

$$= V + V(\alpha+\beta)GV + \cdots \qquad 2.24$$

Regrouping Y gives

$$Y = L + L\beta G L + L\beta G L \beta G L + \cdots \qquad 2.25$$

where

$$L = V + V\alpha G L + \cdots \qquad 2.26$$

Equation (2.26) shows that the intermediate states are all such that the target and incident particles are excited. However, in the series (2.25) all the intermediate states of the target nucleus are ground states, only the incident nucleon being excited.

The potential V is taken to be the sum of two-body

interaction potentials, namely

$$V = \sum_{i=1}^{A} v_i \qquad 2.27$$

At this stage we introduce a two-body operator t_i:

$$t_i = v_i + v_i \alpha G v_i + \cdots \qquad 2.28$$

$$= v_i + v_i \alpha G t_i \qquad 2.29$$

The operator t_i represents the scattering of the incident particle by the i^{th} target nucleon. This operator is not equal to the "free" transition operator T in the usual sense due to the presence of αG factor. However, at high energies the impulse approximation is assumed to be valid, hence these two exprssions become the same.

Now substitute (2.25) into (2.22) after a direct expansion. We obtain

$$\langle U \rangle = \langle L \rangle \qquad 2.30a$$

or

$$\langle U \rangle = \langle | \sum_i t_i + \sum_i \sum_{j \neq i} t_i \alpha G t_j + \cdots | \rangle \qquad 2.30b$$

In the series (2.30) we can see the Optical Potential as being represented by a series of two-body interaction

potentials. The first term of the series is

$$\langle \vec{k}' | \sum_i t_i | \vec{k} \rangle \qquad 2.31$$

where $\vec{k}$ is the initial and $\vec{k}'$ is the final momentum in the center of mass system of particle and nucleus. If we assume the validity of the Impulse Approximation and complete anti-symmetrization of the ground state wave function of the target nucleus, then all the terms in the sum are equal and (2.31) can be written as

$$\begin{aligned} \langle \vec{k}' | \sum_i t_i | \vec{k} \rangle &= A \langle \vec{k}' | t_0 | \vec{k} \rangle \\ &= \frac{A}{(2\pi)^3} \int d\vec{P}\, d\vec{P}'\, d\vec{\mu}\, \psi^*_{\xi_0}(\vec{\mu}, \vec{P}') \\ &\quad \times \langle \vec{P}', \vec{k}' | t_0 | \vec{P}, \vec{k} \rangle \psi_{\xi_0}(\vec{\mu}, \vec{P}) \end{aligned} \qquad 2.32$$

where $\vec{P}$ and $\vec{P}'$ are the initial and final values of the momentum co-ordinate of the target nucleon. The symbol ξ_0 denotes the remaining A-1 momentum co-ordinates which we assume to be unchanged by the collision. Before we proceed further, we should point out that the essential approximation done here is to replace t_i, the effective two-body operator, by t_0, the transition operator for the scattering of two-free nucleons.

For high energies the dependence on the motion of the target nucleon can be neglected and the matrix element of t_0 is given by:

$$\langle \vec{P}', \vec{k}' | t_0 | \vec{P}, \vec{k} \rangle = \langle \vec{k}' | t_0 | \vec{k} \rangle \delta(\vec{P}' + \vec{k}' - \vec{P} - \vec{k}) \quad . \tag{2.33}$$

Substituting (2.33) into (2.32), we have

$$\frac{A}{(2\pi)^{3A}} \int d\vec{\mu}\, d\vec{P}\, \Psi^*_{\xi_0}(\vec{\mu}, \vec{P} - \vec{q}) \langle \vec{k}' | t_0 | \vec{k} \rangle \Psi_{\xi_0}(\vec{\mu}, \vec{P}) \tag{2.34}$$

where $\vec{q} = \vec{k}' - \vec{k}$, is the momentum transfer. The Fourier Transform of the target wave function $\Psi_{\xi_0}(\vec{n}', \vec{r}')$ to momentum space is

$$\Psi_{\xi_0}(\vec{\mu}, \vec{P}) = \int d\vec{n}'\, d\vec{r}'\, \Psi_{\xi_0}(\vec{n}', \vec{r}')\, e^{-i(\vec{P}\cdot\vec{r}' + \vec{\mu}\cdot\vec{n}')} \tag{2.35}$$

and implies that (2.32) can be written as:-

$$\langle \vec{k}' | U | \vec{k} \rangle = A \langle \vec{k}' | t_0 | \vec{k} \rangle \int d\vec{n}'\, d\vec{r}'\, e^{-i\vec{q}\cdot\vec{r}'} |\Psi_{\xi_0}(\vec{n}', \vec{r}')|^2$$

$$= A \langle \vec{k}' | t_0 | \vec{k} \rangle \int d\vec{r}'\, \rho(\vec{r}')\, e^{-i\vec{q}\cdot\vec{r}'} \tag{2.36}$$

where

$$\rho(\vec{r}') = \int d\vec{n}'\, |\Psi_{\xi_0}(\vec{n}', \vec{r}')|^2 \tag{2.37}$$

and ρ is the onebody density distribution normalized by:-

$$\int \rho(\vec{r}')\, d\vec{r}' = 1 \quad . \qquad 2.38$$

If U is local and energy dependent, then

$$\langle \vec{k}' | U | \vec{k} \rangle = \int d\vec{r}'\, U(k,\vec{r}')\, e^{-i\vec{q}\cdot\vec{r}'} \qquad 2.39$$

and for $\vec{q} = 0$

$$\int d\vec{r}'\, U(k,\vec{r}') = A\langle \vec{k}' | t_o | \vec{k} \rangle \quad . \qquad 2.40$$

Hence, we can see the volume integral of the optical potential is simply related to the nucleon-nucleon scattering amplitude.

To understand the significance of the imaginary potential, consider $\vec{q} = 0$; the forward scattering amplitude is given by

$$f(0) = \frac{-m}{4\pi} \langle \vec{k} | t_o | \vec{k} \rangle \qquad 2.41$$

By the Optical theorem, we have

$$\mathrm{Im}f(0) = \frac{m\sigma}{8\pi} |\vec{V}| \quad . \qquad 2.42$$

where V is the relative velocity of the colliding nucleons and is the effective total nucleon-nucleon cross-section

averaged over neutrons and protons. Equating (2.42) and (2.41)

$$\mathrm{Im}\left(\frac{-m}{4\pi}\langle\vec{k}|t_o|\vec{k}\rangle\right) = \frac{m\sigma}{8\pi}|\vec{V}| \qquad 2.43$$

or

$$\mathrm{Im}\left(\frac{-U(k,\vec{r})}{A\rho(r)}\right) = \frac{\sigma|\vec{V}|}{2} \qquad 2.44$$

which implies

$$-\mathrm{Im}\,U(k,\vec{r}') = \frac{A\sigma\rho(r)|\vec{V}|}{2} \qquad 2.45$$

$$= \frac{A|\vec{V}|}{2\lambda} \qquad 2.46$$

where ρ is the nucleon density for the target nucleus. We can see that the imaginary potential is simply related to the mean free path λ inside the nuclear matter. However, one should note that the Exclusion Principle has not been accounted for here. A detailed treatment has been given by Lane et al. (LA65).

CHAPTER 3

METHOD OF ANALYSIS

3.1 Optical Potential Model

The $P+^4He$ elastic scattering data in the medium energy range (100 MeV $\leq$ Ep $\leq$ 1000 MeV) are analyzed using the Optical Potential Model. The target nucleus is assumed to be spherical and to have spin-0. This Optical Model Potential is an approximation to the true potential which represents the Optical Model Operator U defined in Chapter 2. The Optical Model Potential used here has the form:

$$V_{opt}(r) = V_c(r) - V_o f_o(r) - iW_v f_v(r) + \frac{2}{r}(V_{s\cdot o} + iW_{s\cdot o}) \frac{df_{s\cdot o}}{dr}(\vec{\ell}\cdot\vec{\sigma}) \qquad 3.1$$

where $V_c(r)$ denotes the coulomb potential due to a uniformly charged sphere of radius R_c and charge Ze:

$$V_c(r) = \frac{Ze^2}{2R_c}\left(3-\left(\frac{r}{R_c}\right)^2 \right) \qquad r \leq R_c$$

$$= \frac{Ze^2}{r} \qquad r \geq R_c \qquad 3.2$$

where the radius R_c is taken to be $1.36A^{1/3}$ fm which is taken to be constant throughout the analysis. The quantity V_o denotes the real central potential and W_v denotes the

volume part of the central imaginary potential. The spin-orbit potential is of the usual Thomas form with $V_{s.o}$ as the real part and $W_{s.o}$ as the imaginary part. The shape of the potential is expressed through a function $f_i(r)$ of the Woods-Saxon form:

$$f_i(r) = [\ 1 + \exp(\frac{r - r_i A^{1/3}}{a_i})\ ]^{-1} \qquad 3.3$$

In general, the radius and diffusness of the form factor are different for different parts of the potential. During the course of our search, we found no evidence of a surface peaked imaginary term, consequently it is not included in equation (3.1) and is not used in the latter part of the analysis.

3.2 Data.

There are a large number of P+⁴He elastic scattering data available for cross-section. However, some of these experimental results have changed very rapidly during the last few years. In order to obtain any meaningful results, we have to discriminate against those data that are known to be inconsistent with other authors work. In table 1 we give a list of experimental data selected for this search.

3.3. Relativistic Corrections

When using the non-relativistic Schrodinger equation to analyze medium energy data, it is necessary to correct for relativistic effects. If these effects were not corrected, the analysis would give misleading information about the potential depth and the geometry. The problem of relativistic corrections could have been avoided if the Klein-Gordon equation or the Dirac equation were used instead of the Schrodinger Equation. Even so, problems still exist. In the first case, if one were to use the Klein-Gordon equation to describe the scattering of spin-1/2 particles scattering off a spin-0 target, then one would have to ignore the spin-orbit effects. The effects of the spin-orbit potential are clearly essential for the reproduction of polarization data as indicated in the lower energy analyses. In particular many authors have pointed out that the spin-orbit force is essential in the analyses of P+⁴He scattering data. A more accurate way to include both spin and relativistic effects is by using the Dirac equation. The Dirac equation with an explicit spin-orbit potential has not yet been solved. There are also ambiguities in the definition of the Optical Potential that have not yet been fully explored.

Elton (EL66, IN74) pointed out that one may correct for the relativistic effects by calculating the wave number 'K' in the center of mass frame using relativistic

kinematics. Such a wave number is given by:

$$K = m_2 \left(\frac{T^{lab}(T^{lab}+2m_1)}{(m_1+m_2)^2 + 2m_2 T^{lab}} \right)^{1/2} \qquad 3.4$$

where m_1 and m_2 are the rest masses of the projectile and target respectively and T^{lab} is the kinetic energy of the incident projectile in the laboratory frame. One then works backward using non-relativistic mechanics to obtain an incident energy to use as a parameter in the automatic search code 'SEEK' (SE65).

3.4. Search Procedure.

In the present analysis of P+⁴He elastic scattering data, the final parameters were determined generally by minimum values of the total chi-square. This quantity is given by:

$$\chi^2 = \chi^2_\sigma + \chi^2_p \qquad 3.5$$

where χ^2_σ is defined as:

$$\chi^2_\sigma = \sum_{i=1}^{N\sigma} \left[\frac{\sigma_{ex}(\theta_i) - \sigma_{th}(\theta_i)}{\Delta\sigma_{ex}(\theta_i)} \right]^2 \qquad 3.6$$

and $\sigma_{ex}(\theta_i)$, $\sigma_{th}(\theta_i)$, and $\Delta\sigma_{ex}(\theta_i)$ are respectively, the experimental, theoretical and experimental error values for

the cross-section at a center of mass angle θ_i . A similar expression holds for the χ_p^2 , the χ^2 associated with the polarization data.

In the beginning of the search, some criteria were set to eliminate some of the ambiguities that might arise from considering a pure minimum χ^2 fit to the experimental data alone. The conditions are :

1.) The calculated reaction cross-section must agree reasonably well with the experimental data whenever it is available(IG67).

2.) Parameters must exhibit a reasonable continuity as a function of the incident proton energy.

3.) Whenever possible, cross-section data and polarization data are analayzed simultaneously.

The first two conditions are used to eliminate any irregular values of the optical model parameters in the search processes. Therefore some fits with smaller value of ^{2} were discarded.

In phencmenological Optical Model analysis, an ideal set of data should contain both polarization and cross-section data for simultanteous analysis. The presence cf polarization data helps to regulate the variations of the spin-orbit term. The desire of having both polarization and cross-section data at the same energy can not be satisfied by all data sets. Therefore to control the variations in spin-orbit potential, we included polarization data from a neighbouring energy with existing cross-section data into

the analysis and vice-versa.

The optical model parameters at 156 MeV found by Comparat et al.(CO75) were used as starting parameters of the analysis. The parameters were improved by the computer code 'SEEK' at 156 MeV. Attempts were made to maintain the improved geometry set at a constant value for different proton energies. This procedure was carried out until reasonable fits to the experimental data could not be obtained by varying the potential parameters alone. In keeping the geometry constant we reduced the number of variables from eleven to four (V_o , W_v , $V_{s\cdot o}$ and $W_{s\cdot o}$). We hope this kind of practice will provide a better picture of energy dependence of Optical Potential parameters.

The improved geometry set obtained from the above procedure failed to reproduce the P+⁴He data above 312 MeV. A new set of geometry was developed by choosing an appropriate set of a_o and r_o to match the r.m.s. radius obtained from e+⁴He elastic scattering data. Final variations were made on a_o ,r_o and other parameters to minimize χ^2 . This new set of geometry was used for proton energies from 500 MeV to 1100 MeV.

For large scattering angles, the Optical Model Potential (3.1) is not able to reproduce the experimental data. In an attempt to remedy this deficiency, a Majorana Exchange Potential term (GR72) is added to the potential.

The Exchange Potential is defined as:

$$V_{ex}(r) = (-1)^{\ell} U_{ex} f_{ex}(r) \quad . \qquad 3.7$$

Now the modified optical potential model is given as:

$$U(r) = V_{opt}(r) + (-1)^{\ell} U_{ex} f_{ex}(r) \quad . \qquad 3.8$$

Initially Optical Model searches on large angle data were performed at 156 MeV by starting with the best fit parameters from the forward angle fit($\theta_{c.m.} \leq 100^{o}$), allowing only the parameters associated with the exchange potential to vary in order to fit the data including the back-angles. After convergence of the χ^2, final variations on all potential parameters were allowed to minimize the χ^2. In general, the final changes were small. The exchange potential geometry obtained is generally kept constant for further analyses. The geometry of the Exchange Potential was allowed to vary only if the geometries of V_{opt} (r) were allowed to change.

Table 1

Data selection for the P+⁴He Optical Model analysis in the energy range 100 - 1150 MeV

Tp (MeV)	Types of data	Reference
100	cross-section	(GO70)
147	polarization	(CO59)
156	cross-section	(CO75)
203	polarization	(GO59)
	& cross-section	
312	polarization	(CH56)
	& cross-section	
350	cross-section	(SC76)
560	cross-section	(KL77)
	& polarization	
650	cross-section	(SC76)
650	cross-section	(BE76)
720	cross-section	(VE75)
720	cross-section	(MC65)
	& polarization	
800	cross-section	(KL77)
	& polarization	
1030	cross-section	(KL77)
	& polarization	
1150	cross-section	(SC76)

CHAPTER 4

RESULTS

The P+⁴He data have been analyzed by the Optical Potential Model. The automatic search for minimum χ^2 was performed by the computer code 'SEEK' (App. 1), which allows automatic search on all parameters. Since we have fixed the geometry parameters in most cases, the number of search parameters are significantly reduced and the cost of the automatic searches is also reduced. The quality of our fits is based on the over all fit to the data set. The total χ^2 is only used as guidance when performing automatic searches. The results obtained from the searches taking into account the criteria discussed in Chapter 3 are detailed in tables 2 and 3. In figures 1 to 16, the theoretical curves calculated from the best fit parameters together with the experimential data are presented at each individual energy.

1.) 100 MeV DATA (Fig. 1)

The data set is taken from Goldstein et al. (GO70). It contains only the differential cross-sections. The starting search parameters were taken from the 156 MeV best fit result. The method used in the search was to consider related parameters in pairs (i.e. V_0 and W_V and, $V_{S\cdot O}$ and $W_{S\cdot O}$ pairs), until the χ^2 converged. The Optical Model calculation gives a good fit to the forward angle data, but an exchange potential is required to reproduce the large

angle data. The Optical Model calculation, including the exchange effects, is shown in fig. 1.

2.) 156 MeV DATA(Figs. 2 and 3)

The 147 MeV polarization data (C059) and the 156 MeV cross-section data (C075) were considered together in the analysis. An exchange term is included for the reproduction of large-angle data (fig. 2). The polarization data at the forward angles are well describe by the calculation, but the calculation can not reproduce the large angle data with the same quality (fig. 3).

3.) 203 MeV DATA (Fig. 4)

The data set is obtained from Gotow et al. (G059). It consists of both cross-section and polarization data. The starting parameters are taken from the 156 MeV best fit result. Using the method described above we find the calculation gives a good representation for both cross-section and polarization data (fig. 4).

4.) 312 MeV DATA (Fig. 5)

The data set is obtained from Chamberlain et al. (CH56) It contains both cross-section and polarization data. The starting parameters are taken from 203 MeV best fit result. The calculation provides a good fit to the data. We should note that for proton energies at 100, 203 and 312 MeV, the number of variables were limited to four only

and the geometry set is the same.

5.) 350 MeV DATA (Fig. 6)

The data set is that of the Saclay Group (SC76). It contains both cross-section and polarization data. The geometry used in the preceeding analyses failed to provide a good fit to the data. A new set of geometry parameters (table 2) were introduced into the search. It was then possible to get a good fit to the data.

6.) 560 MeV DATA (Figs. 7 and 8)

The 560 MeV data set (KL77) contains both cross-section and polarization data. Using the method described before, we find the calculation gives good fits to both the cross-section data and up to the first minimum ($-t = -.2(GeV/C)^2$) for polarization data.

7.) 650 MeV DATA (Fig. 9)

The data set includes two separate sets of cross-section data. The forward angle data is from Aslanides et al. (SC76) and the back-angle data is from Berger et al. (BE76). The calculation gives fair agreement with the data by including the exchange effects (fig. 9).

8.) 720 MeV DATA (Figs.10 and 11)

The data set is made up of two cross-section data sets and a set of polarization data (VE75, MC65). Employing the

usual method, we find the calculation gives an excellent fit to the cross-section data. A fair agreement is also obtained for the experimental polarization data.

9.) 800 MeV DATA (Figs. 12 and 13)

The data set includes both cross-section and polarization data (KL77). By using the best fit parameters from 720 MeV as starting parameters we were able to obtain a good fit to the cross-section data and a fair agreement for the polarization data.

10.) 1030 MeV DATA (Figs. 14 and 15)

The data set includes both cross-section and polarization data (KL77). Taking the 800 MeV best fit results together with the usual search method, we find the calculation provides good fit to the cross-section and small angle polarization data ($t \leq -.2 (GeV/C)^2$).

11.) 1150 MeV DATA (Fig. 16)

The data set contains cross-section data (SC76) only. By the usual method of calculation excellent fit to the data is obtained. For proton energies at 560, 650, 720, 800, 1030 and 1150 MeV the search parameters were limited to four and an extra degree of freedom (Exchange Potential) was added for the fitting of large angle data.

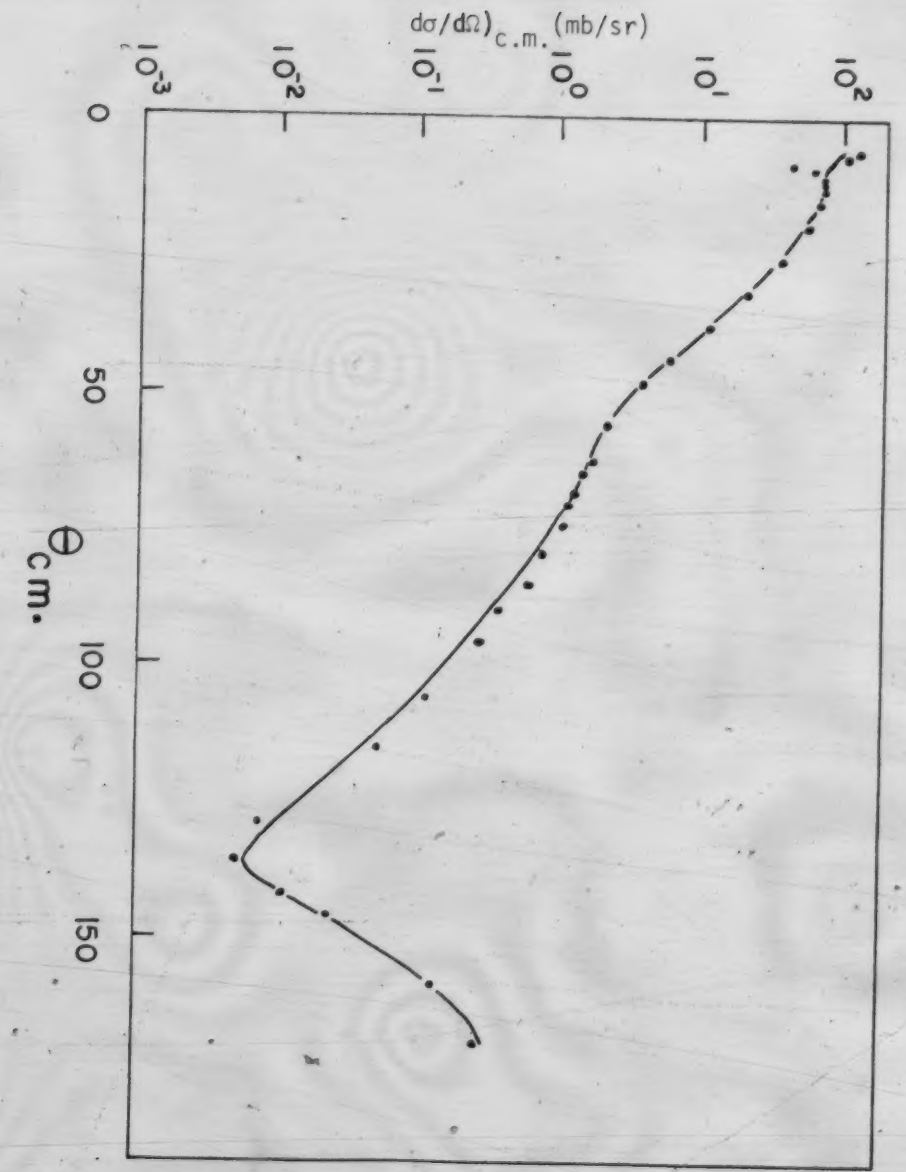

Fig 1. Optical Model fit to 100 MeV data.

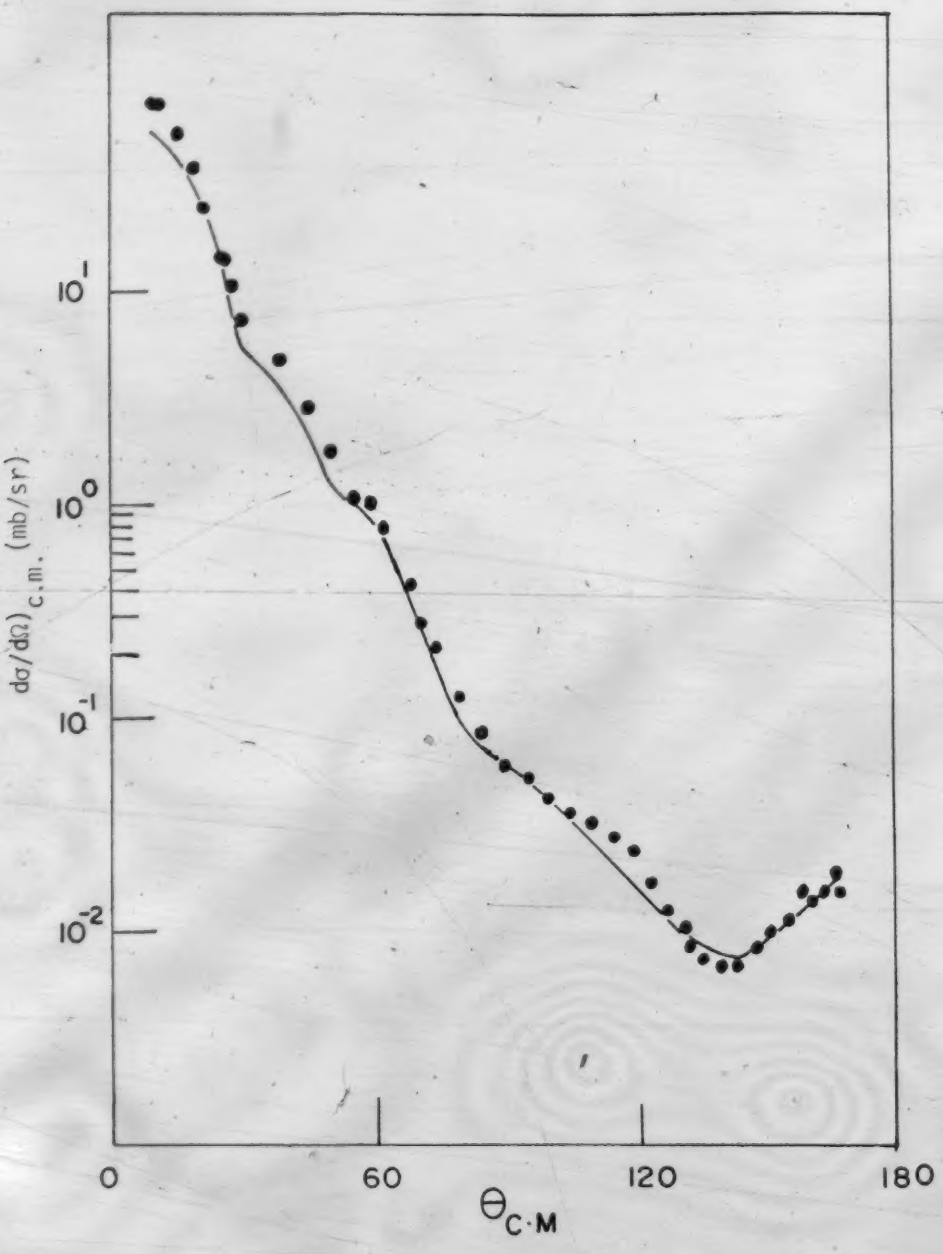

Fig 2. Optical Model fit to 156 MeV cross-section data.

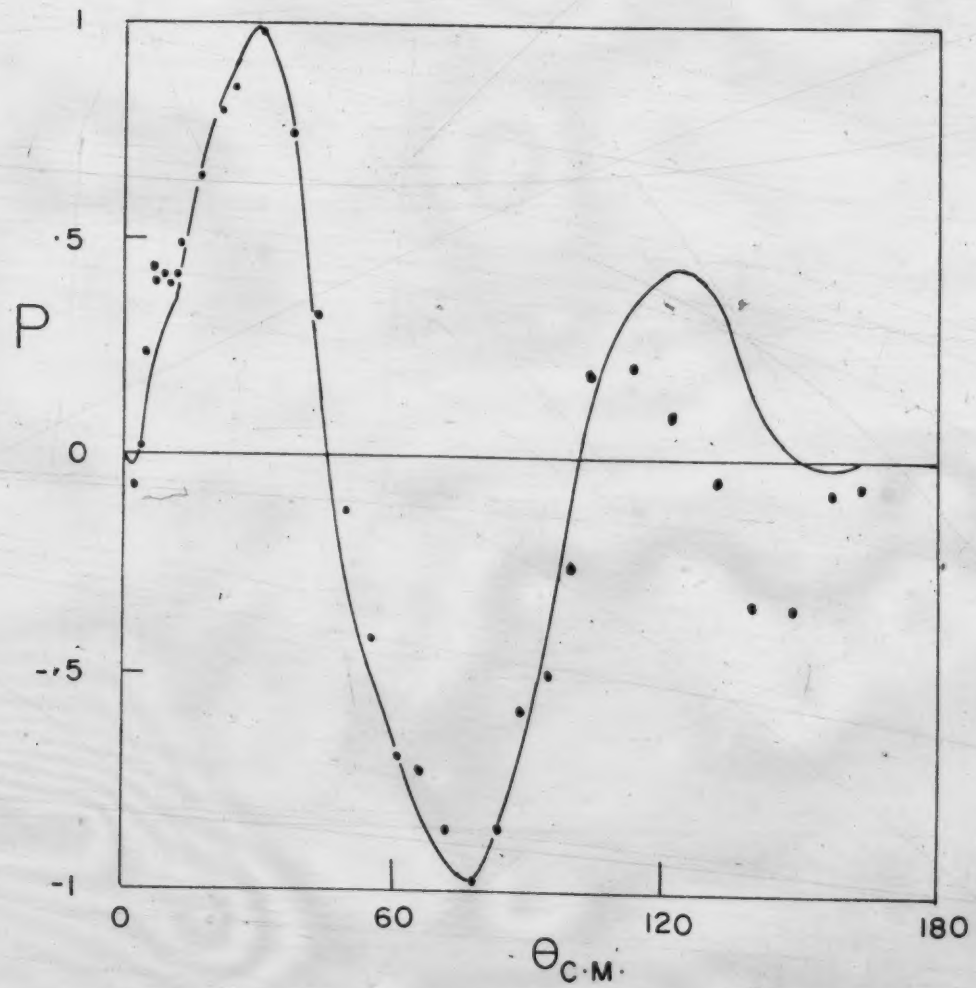

Fig 3. Optical Model fit to 147 MeV polarization data

The theoretical curve is calculated for E_p=156 MeV

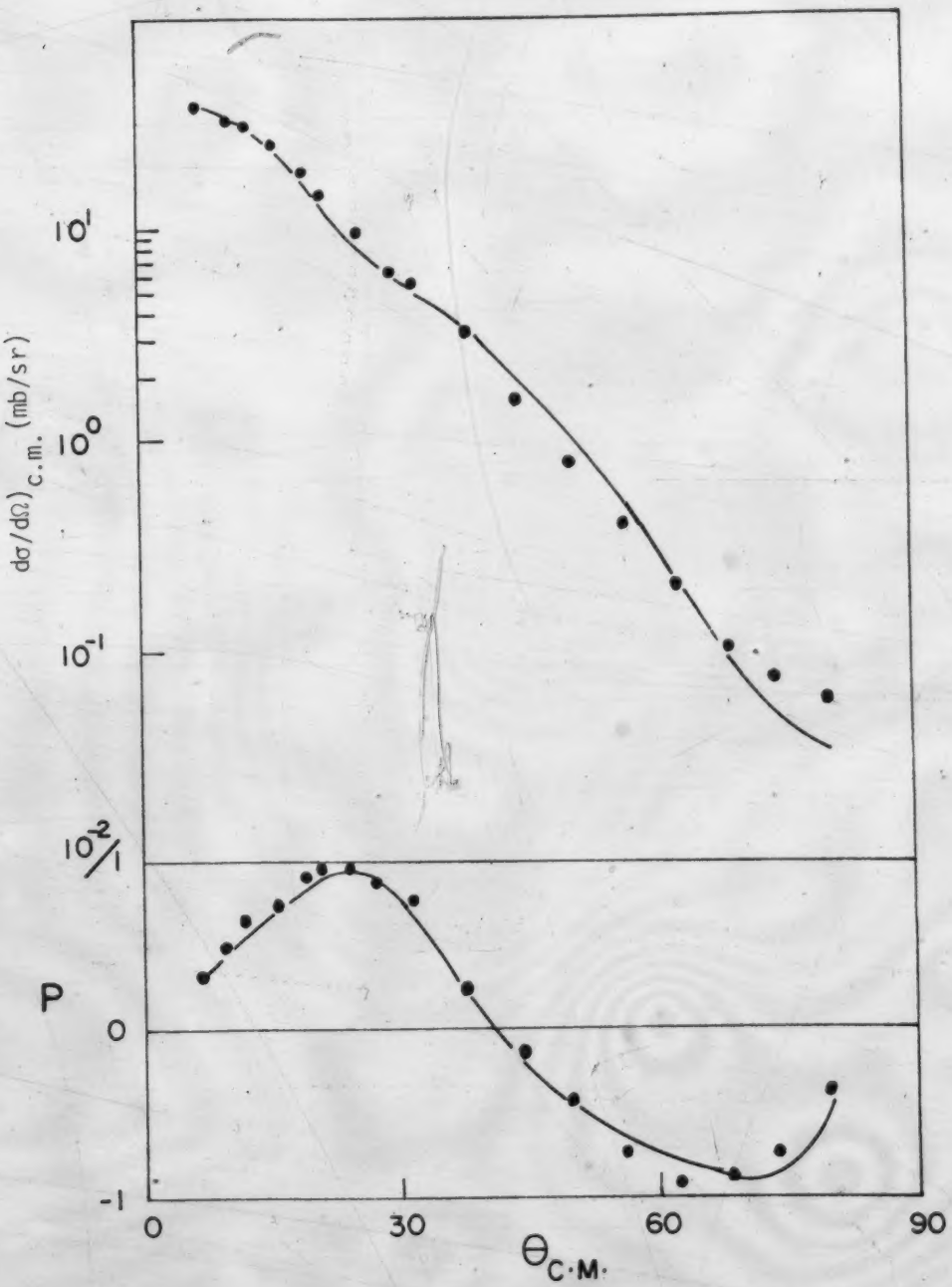

Fig 4. Optical Model fit to 203 MeV data.

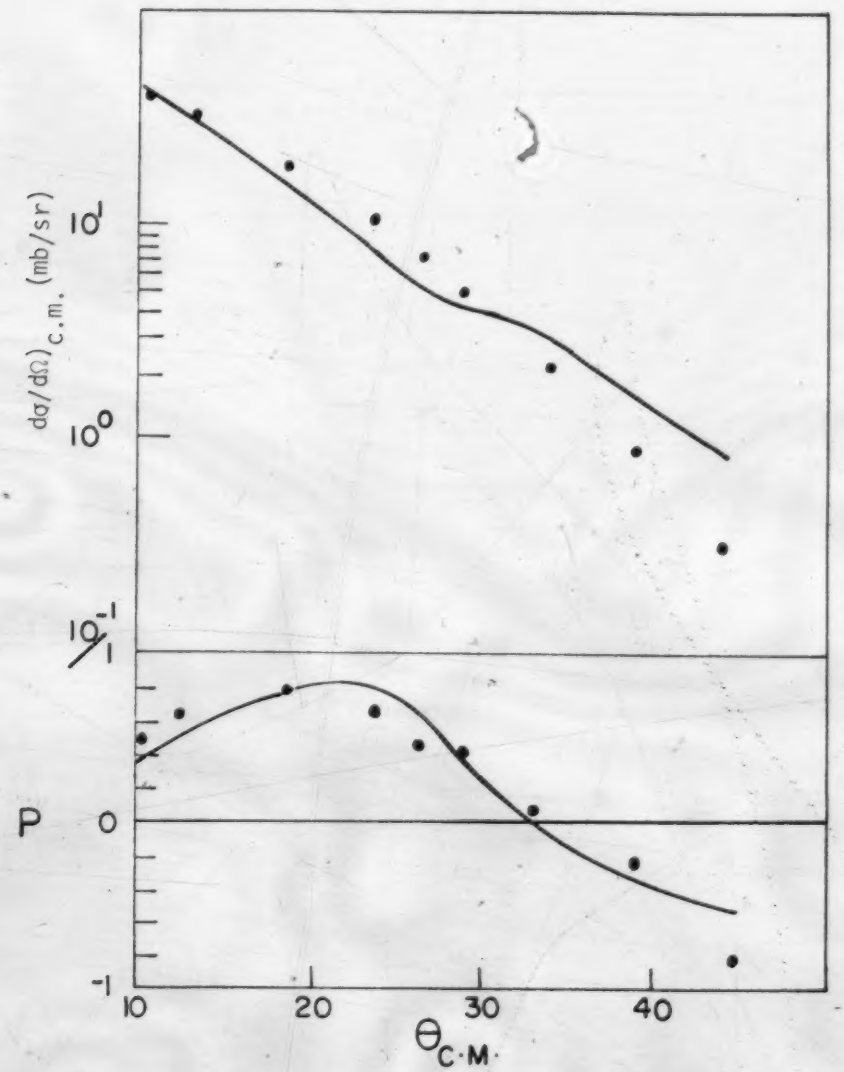

Fig 5. Optical Model fit to 312 MeV data.

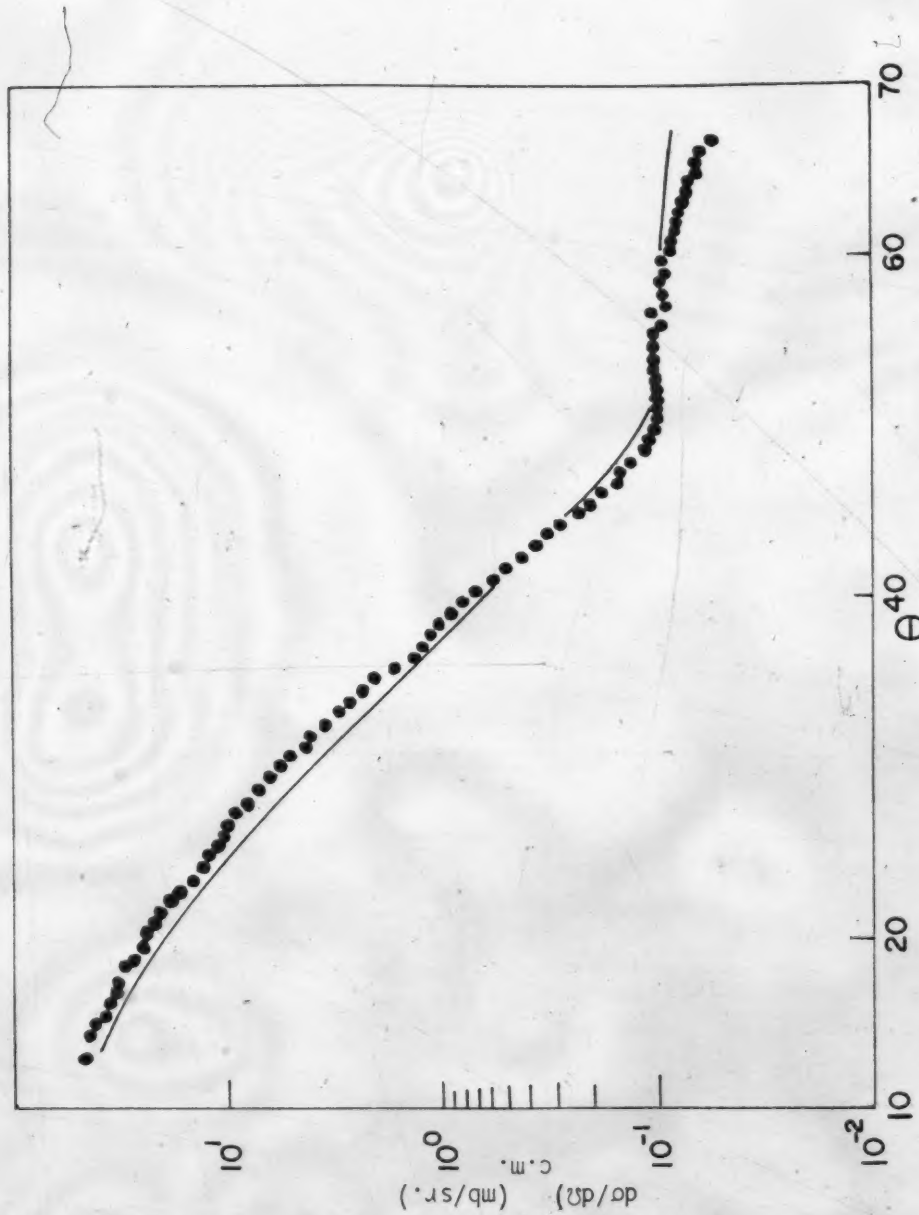

Fig 6. Optical Model fit to 350 MeV data.

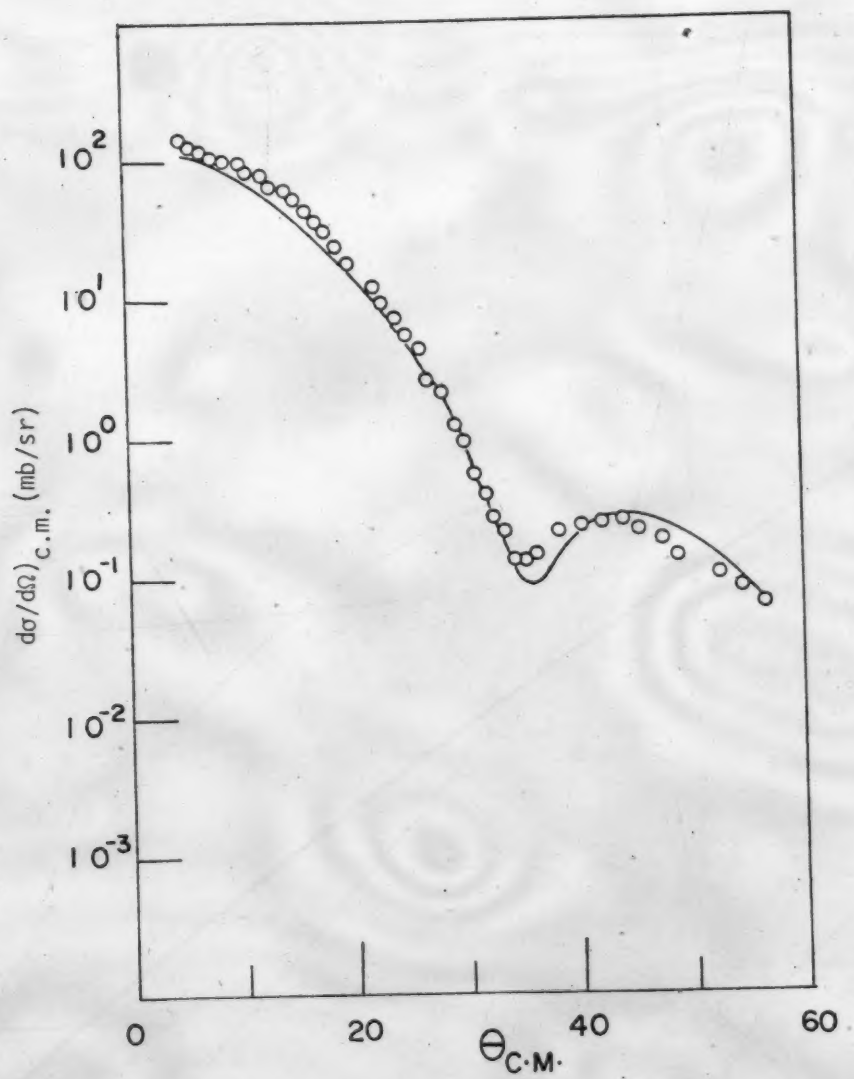

Fig 7. Optical Model fit to 560 MeV cross-section data.

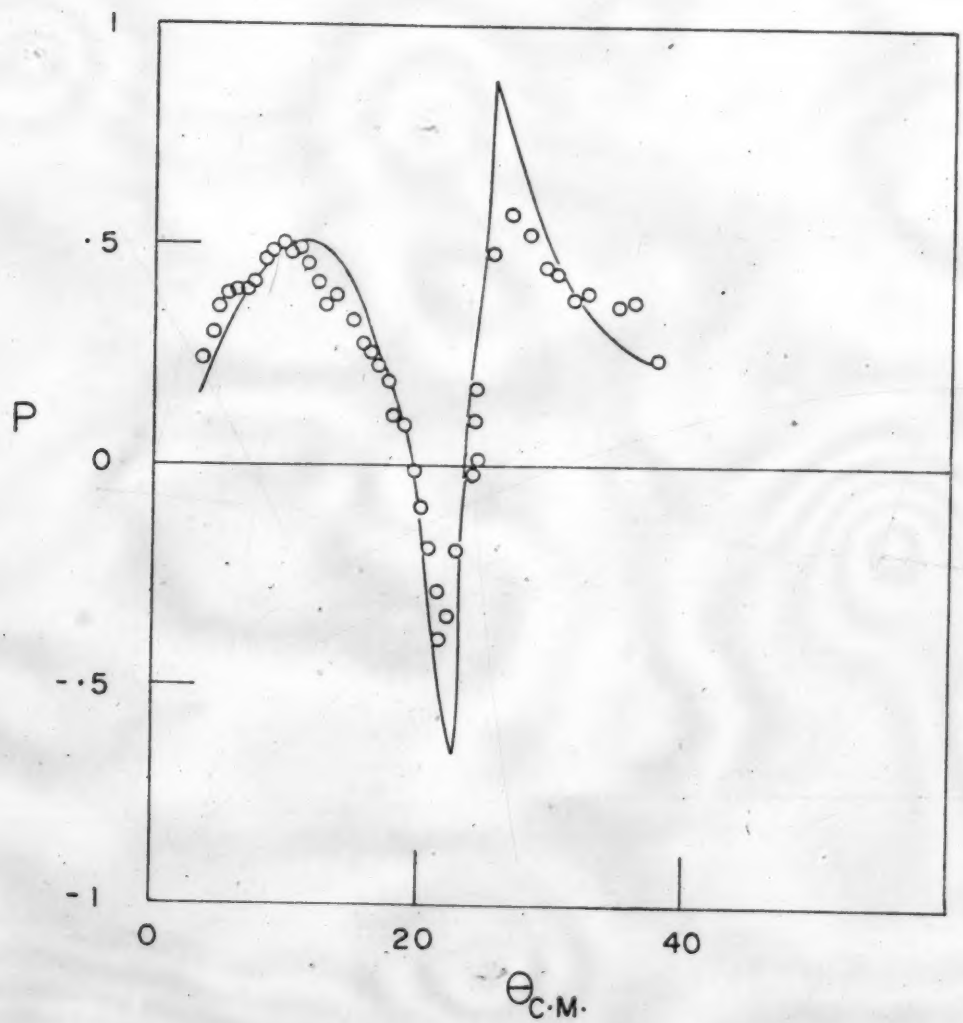

Fig 8. Optical Model fit to 560 MeV polarization data.

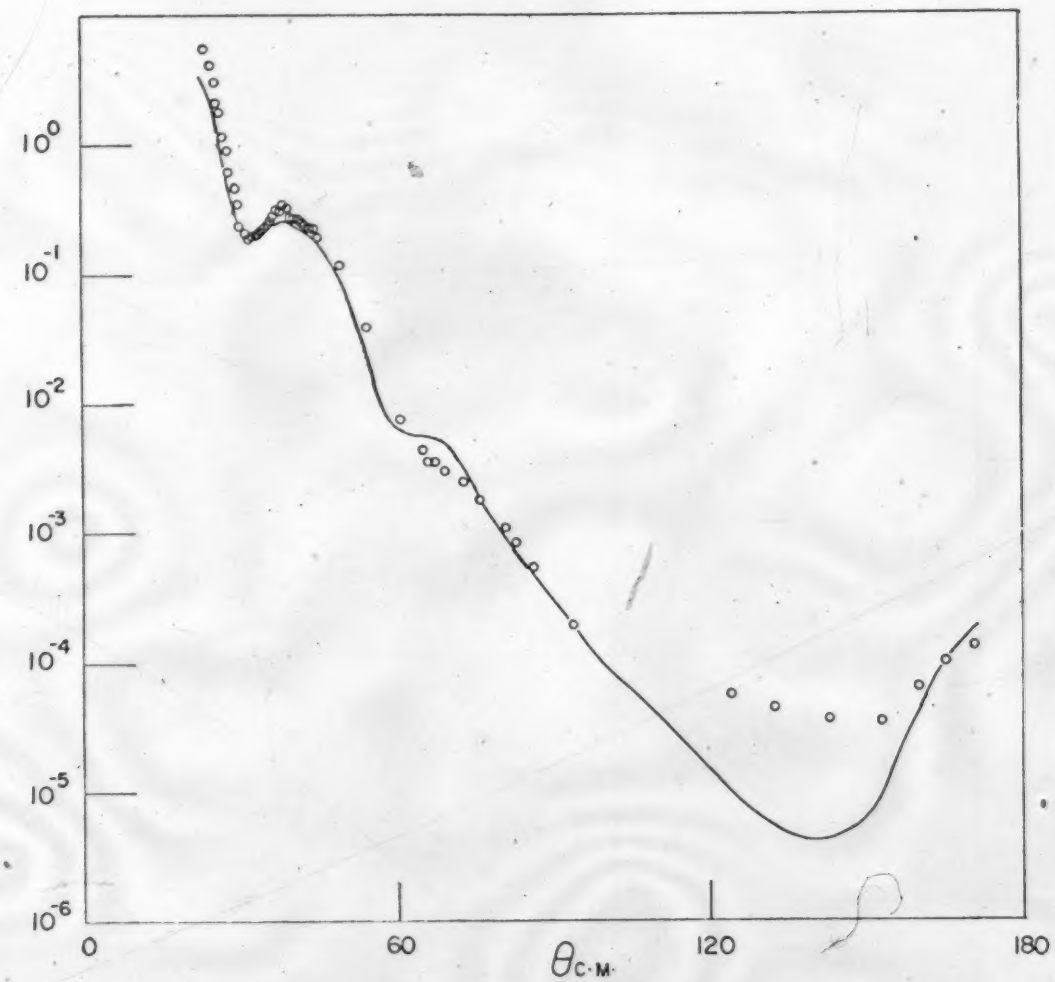

Fig 9. Optical Model fit to 650 MeV data.

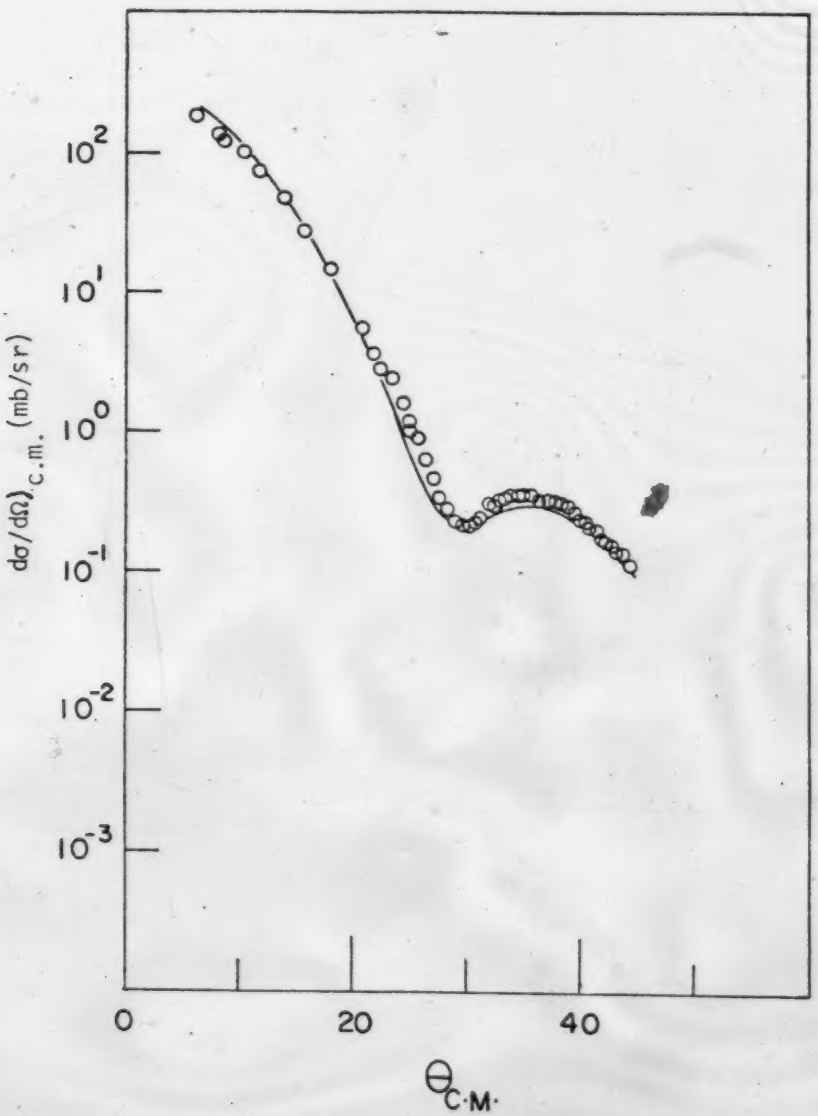

Fig 10. Optical Model fit to 720 MeV cross-section data.

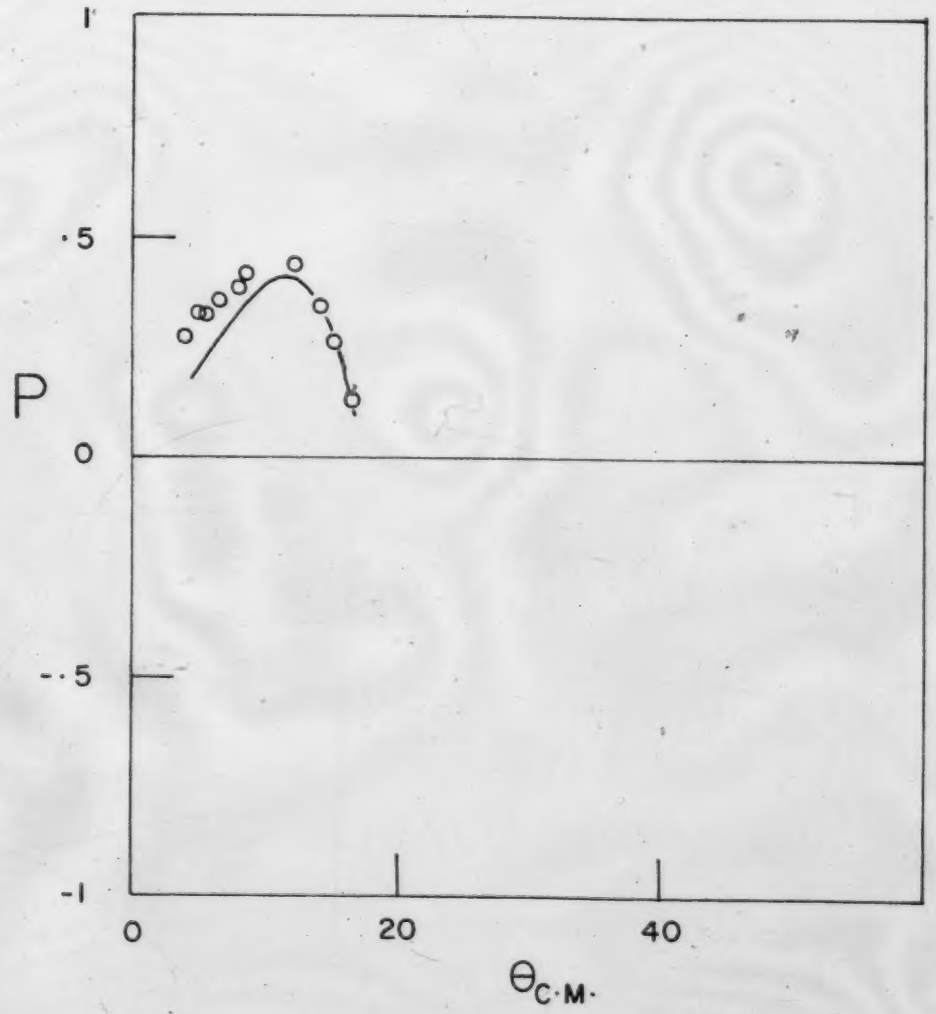

Fig 11. Optical Model fit to 720 MeV polarization data.

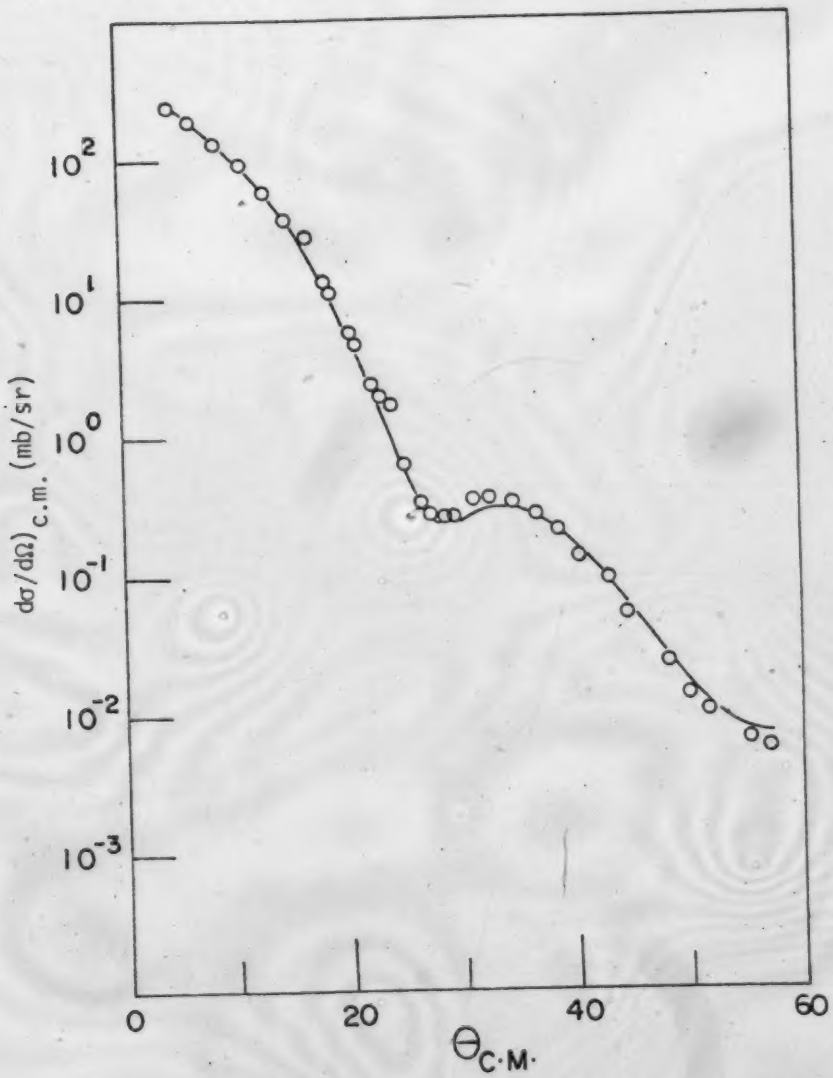

Fig 12 Optical Model fit to 800 MeV cross-section data.

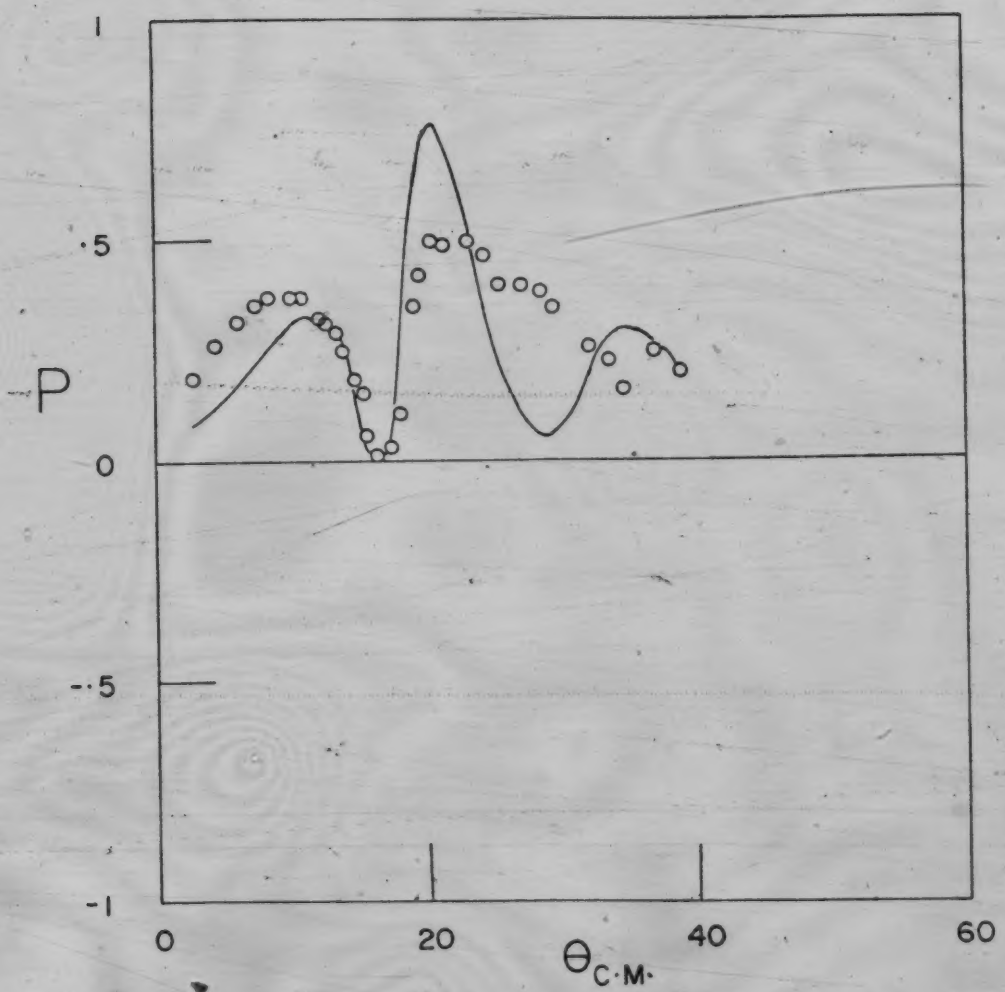

Fig 13. Optical Model fit to 800 MeV polarization data.

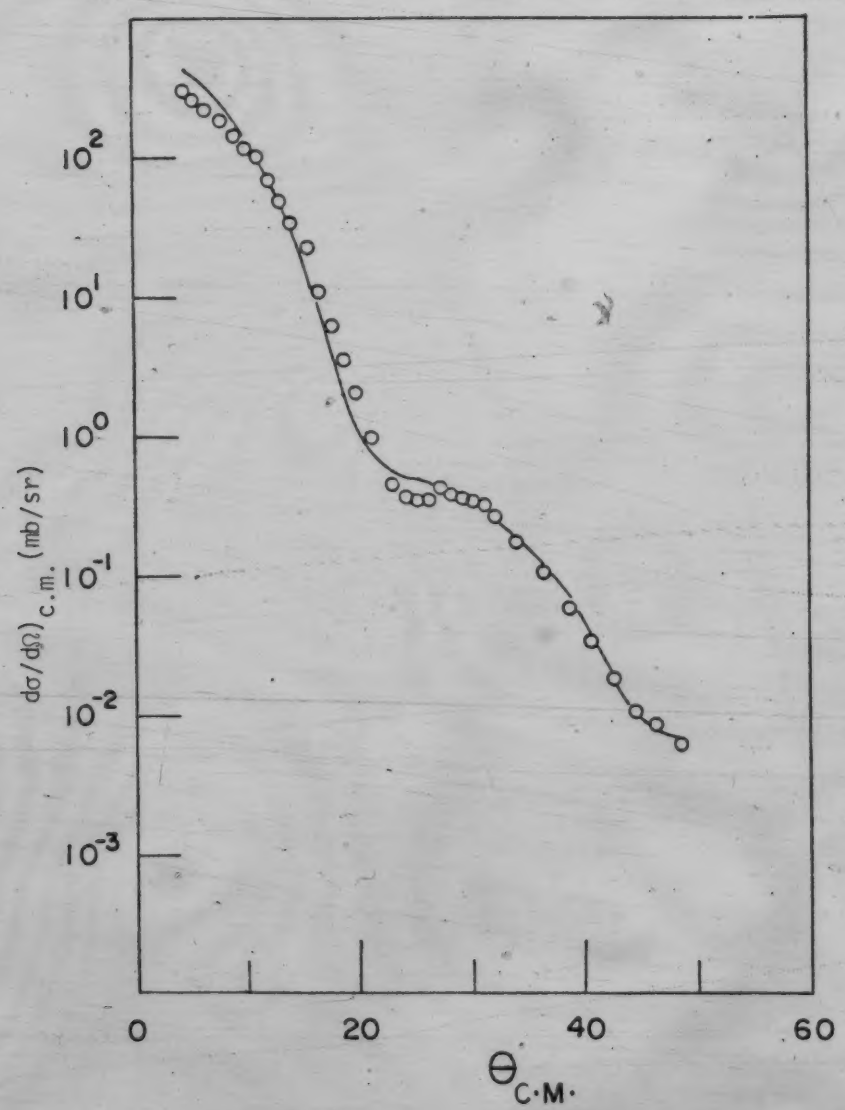

Fig 14. Optical Model fit to 1030 MeV crOss-section data.

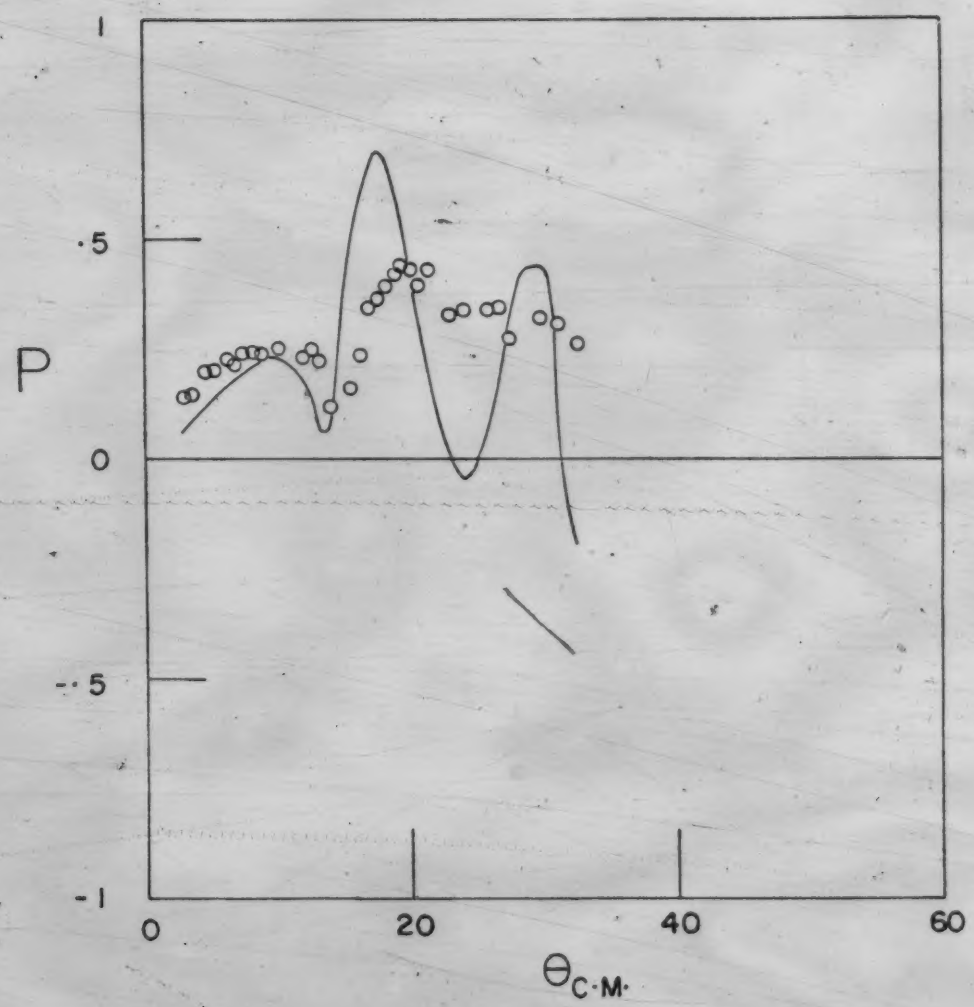

Fig 15. Optical Model fit to 1030 MeV polarization data.

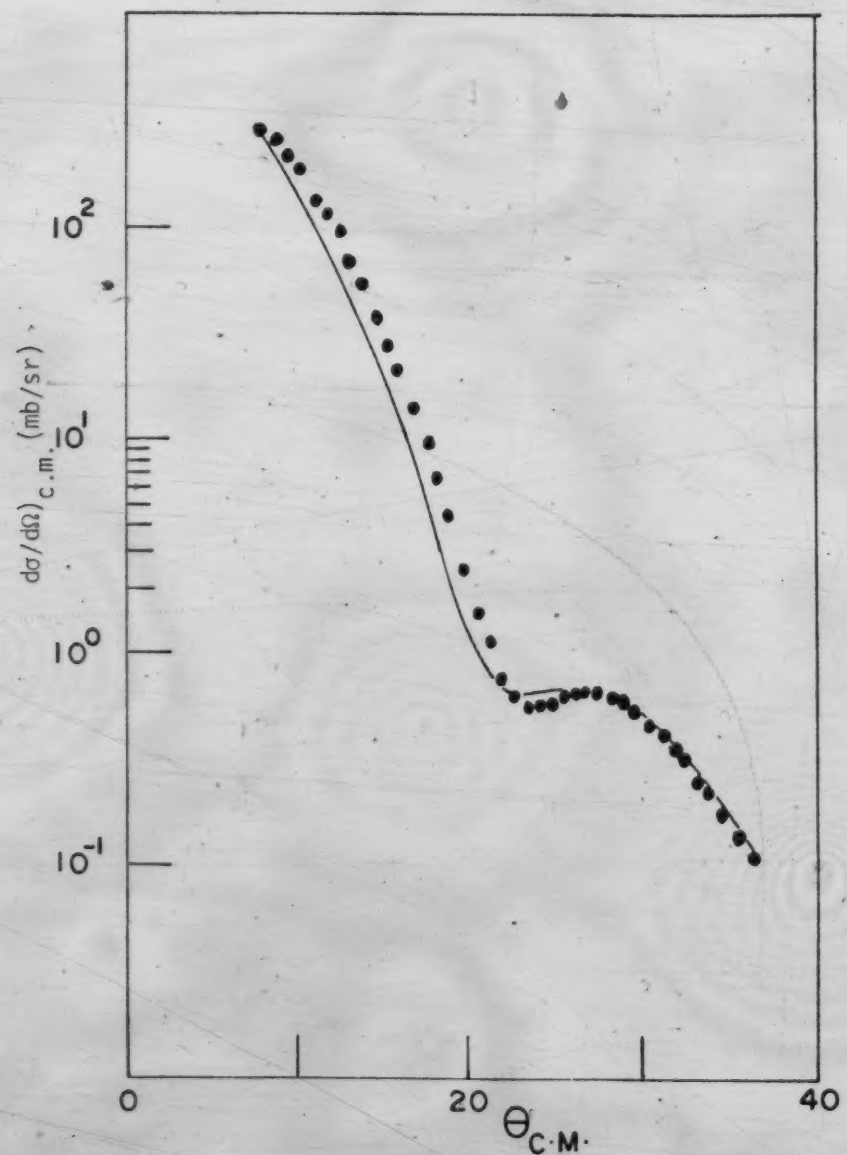

Fig 16. Optical Model fit to 1150 MeV data.

Table 2

Optical Model Geometry

For Ep = 100 to 312 MeV

a_o =0.68 fm a_i =0.317 fm $a_{s.o}$ =.265fm a_{ex} =.408fm

r_o =1.56 fm r_i =1.540 fm $r_{s.o}$ =.802fm r_{ex} =1.54fm

r_c =1.36 fm r.m.s. = 3.073 fm

For Ep=350 MeV

a_o =0.322fm a_i =0.305fm $a_{s.o}$ =.226fm

r_o =1.064fm r_i =1.111fm $r_{s.o}$ =0.831fm

r_c =1.36 fm r.m.s. = 1.773 fm

For Ep=440 to 1150 MeV

a_o =0.134fm a_i =0.342fm $a_{s.o}$ =0.275fm a_{ex} =0.16fm

r_o =1.047fm r_i =1.117fm $r_{s.o}$ =0.895fm r_{ex} =1.04fm

r_c =1.36 fm r.m.s. = 1.38 fm

Table 3

Optical Model Parameters

Ep (MeV)	V_0 (MeV)	Wv (MeV)	Vs.o (MeV)	Ws.o (MeV)	Vex (MeV)	Jr/A MeV-fm^3	Ji/A MeV-fm^3
100	6.98	13.29	12.71	o.	-1.44	185	237.1
156	6.16	12.17	7.88	-5.09	.163	163	217.1
203	3.45	10.31	6.08	-3.69		91.4	183.9
312	2.22	14.78	4.23	-4.42		58.87	263.4
350	2.08	37.81	3.76	-3.47		14.26	281.3
560	-3.65	50.64	2.99	-5.69		-18.89	406.4
650	-7.34	64.64	3.42	-4.32	-.15	-37.99	518.7
720	-8.38	80	2.52	-5.24		-43.38	642.0
800	-11.22	86	1.91	-4.5		-58	690.2
1030	-19.02	115	1.85	-4.92		-98.45	922.8
1150	-42	127.9	3.	-5.83		-217.4	1026.5

CHAPTER 5

DISCUSSION AND CONCLUSION

The results of the Optical Model analyses were detailed in chapter 4. In this chapter we will discuss the results obtained and compare them with the results from other methods of analysis.

5.1 Comparison

Goldstein et al. (GO70) used the Optical Potential to analyze the 100 MeV data, the same method was employed by Comparat et al. (CO75) for proton energies 100 and 156 MeV. The latter also incorporated the 147 MeV polarization data with the 156 MeV cross-section data to control the spin-orbit variations. The Optical Potential parameters obtained by these authors are listed in table 4. The quality of their fits obtained are comparable with our results and some general trends are observed.

1.) The exchange potential is necessary for the reproduction of the large angle data.

2.) The sign of the exchange potential is negative around 100 MeV.

3.) The r.m.s. radius obtained for the exchange potential is larger than the r.m.s. radius for the real central potential.

Comparat et al. (CO75) obtained quality fits using either a pure volume absorption potential or a pure surface

absorption potential for the 156 MeV data. This result indicates the Optical Model has no preference between the surface absorption or the volume absorption potential in this energy range.

Dymartz et al. (DY77) analyzed the data at 350, 440, 650 and 1050 MeV by an 'extended' Glauber Model. The theory takes advantage of the fact that the Optical Potential and the Glauber profile function can be related through Bessel and Abel transforms. The scattering amplitude may be expressed in the form of the impact parameter in the Fourier - Bessel integral which is given as:

$$F(q,p) = \frac{ip}{4\pi} \int d^2b \; e^{i\vec{q}\cdot\vec{b}} \Gamma(\vec{b}) \qquad 5.1$$

where $\vec{p}$, $\vec{q}$ are the incident c.m. momentum and the momentum transfer, respectively. In the Eikonal Approximation the scattering profile function $\Gamma(\vec{b})$ can be simply related to the interaction potential $V(r)$:

$$\Gamma(\vec{b}) = 1 - \exp\left[\frac{-i}{v} \int V(\vec{b},Z)\, dZ \right] . \qquad 5.2$$

For a spherically symmetric potential,

$$V(r) = \frac{iv}{\pi} \int \frac{dZ\; \Gamma'(\sqrt{r^2+Z^2})}{1 - \Gamma(\sqrt{r^2+Z^2})} . \qquad 5.3$$

However, for elastic scattering of an elementary particle on the composite nucleus in the Glauber model (GL59) $\Gamma(b)$ is given by

$$\Gamma(b) = 1 - \langle\Psi| \prod_{j=1}^{A} [\, 1 - \gamma_j(\vec{b}-\vec{s}_j)]|\Psi\rangle \qquad 5.4$$

where γ_j is the individual profile function for target nucleon j, $\vec{s}_j$ being their position in the plane of impact parameters and Ψ is the nuclear target ground state wave function. They evaluate the profile function described in Eq. (5.4) and work backward to obtain a corresponding optical potential. The potential obtained is then inserted into the Schrodinger Equation to obtain the 'exact' scattering matrix. Using a Gaussian form factor for ^{4}He and a spin and iso-spin independent profile function these authors reproduce the forward angle data extremely well for proton energies at 350, 650, and 1050 MeV, However, only a qualitative fit was obtained for 440 MeV data. The quality of their results agrees very well with our results at the forward angles. Since they did not include any exchange effects in their analysis they failed to reproduce the large angle data completely. These authors also compared their results with the standard Glauber Model calculations and found that the latter produces too deep a minimum.

Kujawski (KU70) used the first and second terms from the Optical Model expansion formulated by K.M.T. (KE59) in the Schrodinger Equation. He combined the 587 MeV

cross-section and 540 MeV polarization data for his analysis at 630 MeV. He also analyzed the 1 GeV data from Palevsky et al. (PA67). Including both spin and iso-spin effects, resonable fits were obtained for the data.

Clark et al. (CL73, AR76, SA73) used a purely phenomenological Optical Potential with only real and imaginary parts :

$$U = (V+iW)f(r) \qquad 5.5$$

with the form factor f(r) given by

$$f(r) = \frac{1 + wr^2/c^2}{1 + \exp(\frac{r-c}{z})} \qquad 5.6$$

where w, c and z are parameters obtained from fitting the electron scattering experiment (FR67). The potential is inserted in the Dirac Equation as the fourth part of a four vector potential, with the vector part of the potential taken to be zero. These authors neglected the spin-orbit effects in their analysis. They fitted the cross-section data at 587, 600, 650, 720, 1050 and 1150 MeV, and obtained excellent results.

Auger et al. (AU76) used the extended Glauber Model by Wallace (WA71), the scattering amplitude is given by

$$F(q) = ikR(q)\int e^{i\vec{q}\cdot\vec{b}} [\, 1 - \{1 - \Gamma(\vec{b}-\vec{s})\rho(\vec{r})\, d^3r\} \qquad 5.7$$

$$x A e^{i\chi_c(b)}]\, d^2b$$

where

$$R(q) = e^{<r^2>q^2/6A} \qquad 5.8$$

is the c.m. correction and the function $X_c(b)$ denotes the Coulomb phase. They used a central Gaussian form factor and a spin-dependent profile function given by

$$\int \Gamma(\vec{b}-\vec{s})\rho(\vec{r})\, d^3r = T(b) + \vec{\sigma}\cdot(\vec{b}\times\vec{k})T_s(b) \qquad 5.9$$

with

$$T(b) = \frac{1}{ik_o}\int J_o(qb)\, A(q)\, S(q) q dq \qquad 5.10$$

and

$$T_s(b) = \frac{1}{k_o}\int J_o(qb)\, C(q)\, S(q) q dq \qquad 5.11$$

where $A(q)$ and $C(q)$ are standard amplitudes from nucleon-nucleon interactions and $S(q)$ is the nuclear form factor. Subsituting the above profile function into the Scattering amplitude

$$F(q) = F_1(q) + \vec{\sigma}\cdot\hat{n}F_2(q) \quad . \qquad 5.12$$

The cross-section and polarization are then given by:-

$$d\sigma/d\Omega = |F_1(q)|^2 + |F_2(q)|^2 \qquad 5.13$$

and

$$P = 2Re(F_1^* F_2) \;/\; \frac{d\sigma}{d\Omega} \quad . \qquad 5.14$$

Auger et al. (AU77) included all the available data from 587 to 650 MeV for their analysis at 600 MeV and also analyzed data at 0.72, 1.15 and 24 GeV. They were able to

reproduce the experimental cross-section data and polarization data up to $t = -.2\,(GeV/c)^2$. Beyond this region the calculation failed to reproduce the shape of the polarization data.

Wallace et al. (WA71, 77) used the extended Glauber model to analyze all the 1 GeV data available. In their calculations, they included the effect of the Δ-intermediate state (Δ is the well known 3-3 resonance in the π-N system, where a fast nucleon becomes a Δ in one collision, then the Δ propagates through the nucleus and returns to a nucleon state in a latter collision thereby re-entering the elastic channel.) in a spin and isospin dependent model. Employing a realistic ^{4}He form factor that fitted the e+^{4}He elastic scattering data, Wallace et al. obtained excellent fits to both cross-section and polarization data.

Rule and Hahn (RU75a,b,c, 76) made an Effective Channel analysis of the P+^{4}He elastic scattering data. The intermediate energy proton-nucleus scattering problem is formulated in terms of coupled equations. In this formulation the effects of the inelastic processes are represented by an average inelastic channel. The theory incorporates approximately the effects of non-locality, energy dependence, re-scattering and absorption of all the inelastic channels. The spin-orbit term has not been included into their analysis. Still, they obtained fair agreement with the data.

For the low energy region Ep ≤ 400 MeV the results obtained in this thesis are comparable to the results obtained by other authors. Higher energy region results by Wallace et al. (WA77) seem to be the best. They are not only able to reproduce the cross-section data but, more important, they also are able to reproduce the polarization data for the whole angular distribution of the available data. The phenomenological method employed by Clark et al. (AR76) for proton energies between 500 MeV to 1100 MeV is also able to provide excellent fits. In some cases their results appear to be better than ours. However, one should be cautious in making any direct comparisons due to the smaller angular range ($t = -.7 (GeV/c)^2$) in their analysis.

5.2 R.M.S. Radii and Volume Integrals.

Greenlees (GR68, 70) and his collaborators performed an extensive analysis on all the optical potential model parameters obtained from different methods of analysis. They concluded that the r.m.s. radius and the volume integral per nucleon of the real central potential are well defined quantities in Optical Model analysis. The volume integral per nucleon J/A is given by:

$$J/A = \frac{1}{A} \int V(r)\, d^3r \qquad 5.15$$

$$= \frac{4\pi}{3} Vr \left(1 + \frac{\pi^2 a_0^2}{r_0^2 A^{2/3}} \right) \qquad 5.16$$

The r.m.s. radius is:

$$\langle r^2 \rangle = \left(\frac{\int r^2 V(r) d^3r}{\int V(r) d^3r} \right)^{1/2} \qquad 5.17$$

$$= \left[\frac{1}{5} (3r_0^2 A^{2/3} + 7\pi^2 a_0^2) \right]^{1/2} \qquad 5.18$$

The Woods-Saxon form factor has been assumed (Eq. 3.3) for both calculations. The above two quantities have been calculated for all the cases considered in the present analysis. The results of these calculations are listed in tables 2 and 3.

The $\langle r^2 \rangle^{1/2}$ takes on three different values, they are 3.173 fm , 1.773 fm and 1.38 fm for energies from 100 to 300 MeV, 350 MeV and from 400 MeV to 1100 MeV, respectively. In fig. 17, we show the $\langle r^2 \rangle^{1/2}$ as a function of proton energy including those from previous investigations. We observe that there is a considerable scatter in the r.m.s. radius data for Ep ≤ 500 MeV. A general downward trend for the r.m.s. radius as a function of energy is noted when comparing our results with the values 2.055 fm obtained by Satchler et al. (SA67), 1.86 fm obtained by Thompson et al. (TH70) from their analyses of Ep from 31 to 55 MeV and the value 1.52 fm obtained by Clark et al. (AR76) for Ep between 500 to 1100 MeV. In the higher energy region, the proton elastic scattering data should be sensitive to the nuclear structure due to the short wave length of the incident proton . Therefore, the r.m.s. radius obtained from

the Optical Model analysis at this energy range should be a good indication of the nuclear size. The result determined in the present analysis (Ep ≥ 400 MeV) is 1.38 fm which, is close to the average value 1.52 ± .06 fm obtained by Clark et al. (AR76). It also agrees well with the value 1.42 fm for the proton matter distribution obtained by Frosch et al. (FR67) and 1.677 ± 0.022 fm obtained by Sick et al. (SI76). During the course of fitting the large angle data we found an interesting feature about the r.m.s. radius of the exchange potential. The r.m.s. radius of the exchange potential is larger than the r.m.s. radius for the central potential. This feature has been observed by some other authors at lower energies. As pointed out by Volta et al. (VO74) this result is in contrast to the One-Channel Resonating Group Theory which predicts a strong and shorter ranged potential. The Exchange Potential used, however, is an over simplification and hence a significant difference in detail should be expected.

Passatore (PA67, 68, 75) used the dispersion relation developed by Feshbach (FE58) to analyze the results from phenomenological optical model analyses, to develop a criterion for showing how much the hypothesis of locality affects the energy dependence of the phenomenological potentials. He concluded that :

1.) The real part of the empirical potential depth $V_0(E)$ is monotonically decreasing with energy and it changes sign around 300 MeV.

2.) The imaginary part of the potential depth $W_i(E)$ is monotonically increasing with energy and goes asymptotically to a constant value around 1 GeV.

Van Oers et al. (VA74, 73) followed the above idea to analyze proton elastic scattering for heavier nuclei using the Optical Potential Model. He found a logarithmic energy dependence for Jr/A given by

$$J_r/A = J_0/A + \beta \ln E_p \qquad 5.19$$

The same relation is also observed by Clark et al. (CL73, AR76) and in the present analysis. In fig. 18 we plot Jr/A against proton energy. The graph clearly indicates a downward trend as a function of energy and crosses Jr/A = 0 around Ep = 450 MeV. This result is in fair agreement with the results obtained by Van Oers' et al. (VA74) from their analyses of heavier nuclei and by Clark et al. (AR76) from their analyses of P+⁴He elastic scattering data from 500 to 1000 MeV.

The volume integral of the imaginary potential Ji/A (fig. 19) displays a temporary decrease as function of energy. This phenomenon only extends up to 312 MeV and then Ji/A rises monotonically as a function of energy. Considering the whole picture, the volume integral for the imaginary potential does show a general trend upward as function of proton energy. Since our results only extend up to 1.1 GeV we can not conclude upon the asymptotic behaviour

of Ji/A as the energy increases.

Agrawal et al. (AG74) analyzed a wide range of nuclei from A = 40 - 208 over the energy range Ep = 9.8 - 61.4 MeV. They concluded that the total (surface and volume) imaginary volume integral per nucleon of the Optical Model is a well defined quantity, in the sense that, it is independent of: a) the form factor and the geometrical parameters employed, b) the mass number of the trget and, c) the energy range cover. The same result was also obtained from a subsequent analysis made by Hodgson (HO76) over a wider range of nuclei. However, it is clear from our result that the analogous conclusion can not be made in the higher energy analysis.

There was a lot of speculation about the necessity to include the spin-orbit potential for Ep ≥ 400 MeV in Optical Model analyses, because of its relative small magnitude compared to the central potentials. We find the strength of the spin-orbit potentials agrees with other authors assertions that they are small compared to the central potentials. But the strength can be enhanced considerably by the spin-orbit coupling term ($\vec{\ell}\cdot\vec{\sigma}$) due to the large number of partial waves required in this energy region. The imaginary spin-orbit term also found necessary in filling the diffraction minimum. Its presence also affects the value of the calculated reaction cross-section. Van Oers et al. (VA74) in their analysis of heavier nuclei found that a sign opposite to the sign for the lower energy spin-orbit

potential was necessary to fit the high energy cross-section data which is in contrast to our result. From the present analysis of polarization data the spin orbit term does not change sign over the energy range covered.

5.3 Conclusion

The Optical Potential Model with a spin-orbit potential does give an adequate representation of P+⁴He elastic scattering data over the energy range between 100 to 1100 MeV. The includsion of an Exchange potential does improve the fit to large-angle data (fig. 20) but due to the lack of complete angular distribution of cross-section data we can not obtain any information about the energy dependence of the Exchange Potential. The r.m.s. radius of the real central potential obtained at the high energy range studied agrees with the values obtained by other authors and the results from electron elastic scattering experiments. The volume integral of the real and the imaginary potentials also agrees with the conclusions made by other authors from different methods of analysis and the prediction by Passatore (PA67b, 68) which is based upon Feshbach's (FE58) dispersion theory.

In this thesis we established that an Optical Potential with an exchange term can provide a resonably good reprsentation for the ⁴He data in the medium energy range. The method of fixed geometeries seems to be more convenient and economical than other methods of analysis. The results

obtained here are very useful for D.W.B.A. calculation in this energy range. It is also possible to use this type of systematic analysis to predict good starting values for phenomenological optical potentials at other energies.

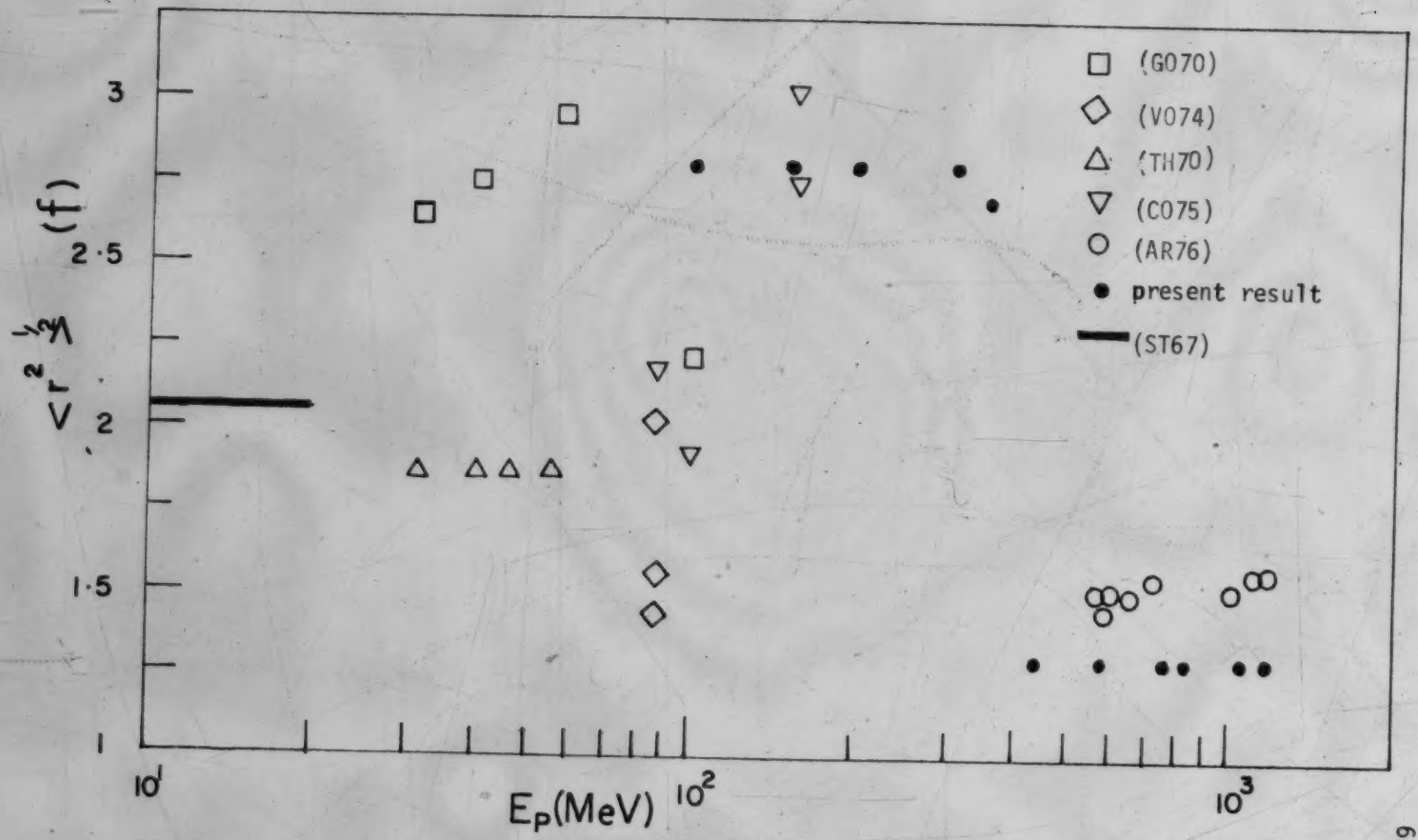

Fig 17. Diagram illustrating r.m.s. distribution with E_p

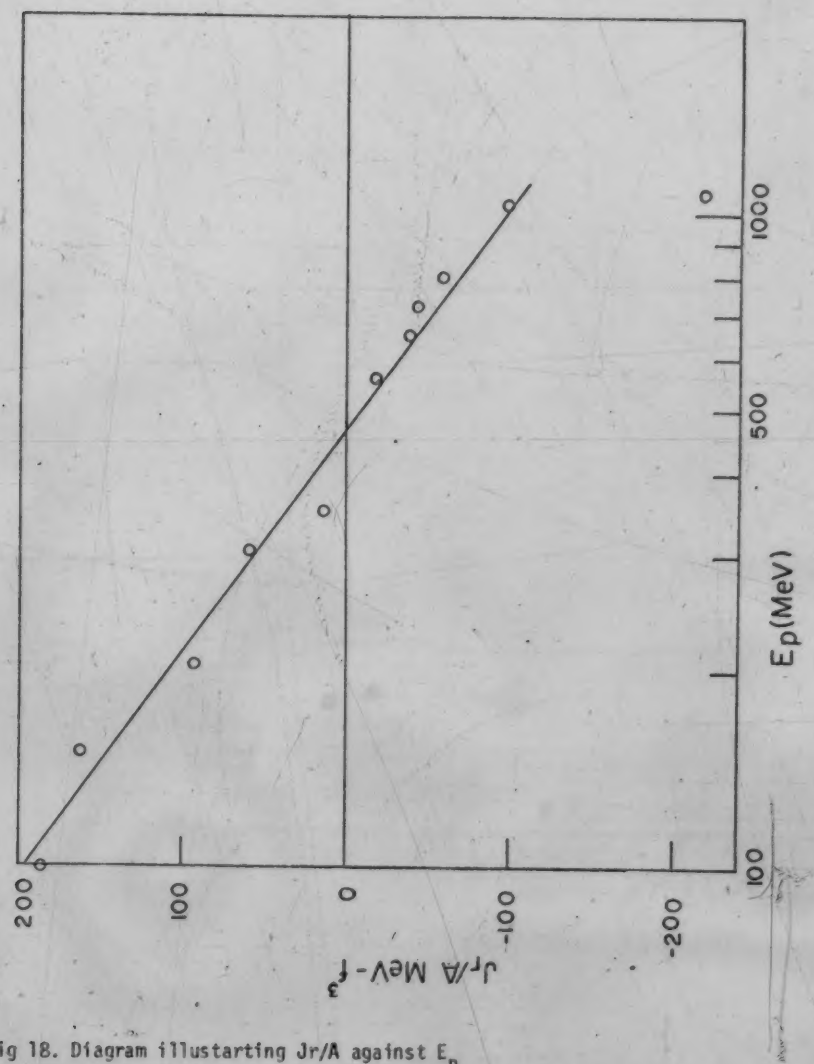

Fig 18. Diagram illustarting Jr/A against E_p

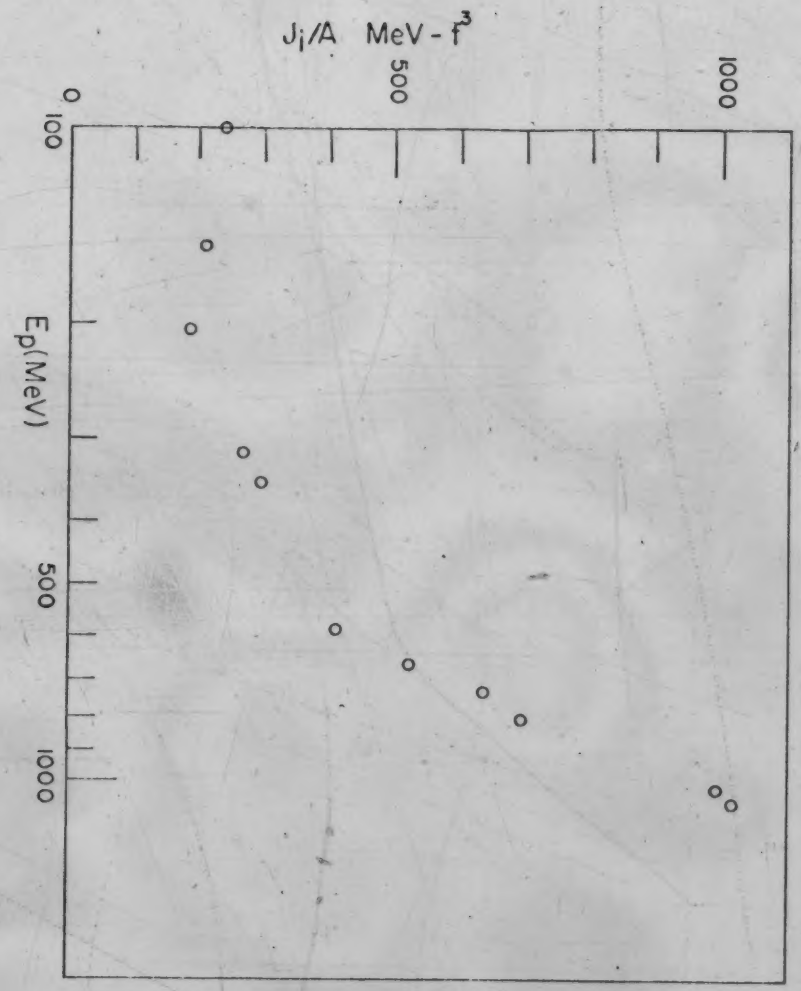

Fig 19. Diagram illustrating Ji/A against E_p

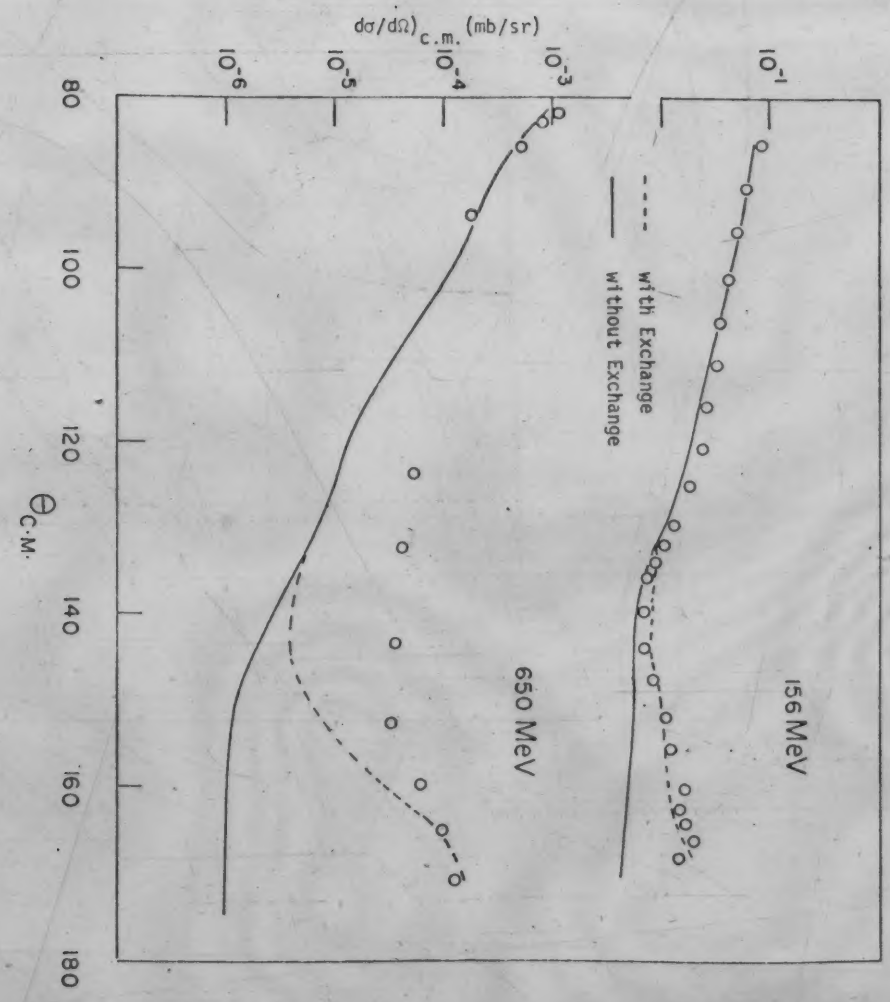

Fig 20. Diagram illustrating the effects of the exchange potential.

Table 4

Optical Model Parameters from other References

Tp (MeV)	Vr (MeV)	Wv (MeV)	Ws (MeV)	Vs.o. (MeV)	Ws.o (MeV)	Vex (MeV)	Ref.
100	11.9	14.8		8.4	.65		(GO70)
100	13.07		8.77	7.53	-6.53	-10.24	(CO75)
156	5.58		15.16	9.69	-7.25	-3.4	(CO75)
156	6.83	12.2		7.72	-5.53	0.	(CO75)
587	31.31	-123.77					(AR77)
650	22.6	-123.3				4.	(AR77)
720	26.17	-128.2					(AR77)
1050	47.22	-126.9					(AR77)
1154	51.31	-126.54					(AR77)

Note Ref.(AR77) has a sign opposite to the convention.

References

AR75 D.C. Agrawal and P.C. Sood, Phys. Rev. C11 (1975) 1854

AR76 L.G. Arnold, B.C. Clark, R.L. Mercer, D.G. Ravenhall and A.M. Saperstein, Phys. Rev. C14 (1976) 1878

AR77 L.G. Arnold, B.C. Clark, R.L. Mercer and D.G. Ravenhall, (private commuication)

BE67 R.H. Bessel and C. Wilkin, Phys. Rev. Lett. 21 (1967) 871

BE68 R.H. Bessel and C.Wilkin, Phys. Rev. 174 (1968) 1179

BE76 J. Berger, J.Duflo, L. Goldzahl, F. Plouin, J. Oostens, M. VanDen Dossche, L.U. Hai, G. Bizard, C. LeBrum. F.L. Fabbri, P.Picozza and L. Satta, Phys. Rev. Lett. 37 (1976) 1195

BO72 E.T. Boshitz, W.K. Roberts, J.S. Vincent, M. Blecher, K. Gotow, P.C. Gugelot, C.F. Perderisat L.W. Swenso and J.R. Priest, Phys. Rev. C6 (1972) 457

CH56 O. Chamberlain, E. Sergi, R.D. Tripp, C. Wiegand and T.Ypsilantis, Phys. Rev. 102 (1956) 1659

CL73 B.C. Clark, R.L. Mercer, D.G. Ravenhall and A.M. Saperstein, Phys. Rev. C7 (1973) 466

CO59 A.M. Cormak, J.M. Palmieri, N.F. Ramsey and R. Wilscn, Phys. Rev. 115 (1959) 599

CO75 V. Comparat, F. Frascaria, N. Fujiwara, N. Marty, M. Morlet, P.G. Roos and A. Willis, Phys Rev. C12 (1975) 251

CZ67 W. Czyz and L. Lesniak, Phys. Lett. 25B (1976) 319

CZ70 W. Czyz, L. Lesniak and L. Woleh, Nul. Phys. B19 (1970) 683

DY77 R. Dymarz and A. Malecki, Phys. Lett. B66 (1971) 413

EL66 L.R.B. Elton, Nuovo Cimento 43 (1966) 277

FE58 H. Feshbach, Ann. Phys. 5 (1958) 357

FE70 H. Feshbach, Ann. Phys. 56 (1970) 268

Fe71 H. Feshbach, A. Gal and J. Hufner, Ann. Phys. 66 (1971) 20

FE73 E. Lambert and H. Feshbach, Ann. Phys. 76 (1973) 80

FR67 R.F. Frosch, J.S. McCarthy, R.e. Rand and M.R. Yearin, Phys. ReV. 160 (1967) 874.

FR68 V. Franco, Phys. Rev. Lett. 21 (1968) 1360

GI59 R.J. Glauber, Lect. Theo. Phys. Ist Ed. W.C. Brittin Wiley Interscience (1959) 315.

GO59 K. Gotow, 1959 Univ. of Rochester Int. Rep. NYO - 2632 (unpublished).

GO68 K. Gotow, E.J. Boshitz, W.K. Roberts, J.S. Vincent, P.C. Gugelot C.F. Perdrisat and L.W. Swenson, Phys. Rev. Lett. 25 (1968) 1816

GO70 N.D. Goldstein, A. Held and D.G. Stairs, Can. J. Phys. 48 (1970) 2629

GR68 G.W. Greenlees, J. Pyle and Y.C. Tang, Phys. Rev. 171 (1968) 1115

GR70 G.W. Greenlees W. Makofske and J. Pyle, Phys. Rev. C1 (1970) 1145

GR72 G.W. Greenlees, W. Makofske, Y.C. Tang and D.R. Thompson, Phys. Rev. C6 (1972) 205

HO76 P.E. Hodgson, Phys. Lett. 65B (1976) 33

IG67 G.J. Igo, J.L. friedes, H. Palevsky, R. Sutter, G. bennett, W.D. Simpson, D.M. Corley and R.L. Stearns, Nul. Phys. B3 (1967) 181

IN74 A. Ingemarson, Physica Scripta Vol. 9 (1974) 156

JO63 P.B. Jones, The Optical Model in Nuclear and Partical Physics. (1963) Interscience Publishers.

KE59 A.K. Kerman, H. McManus and R.M. Thaler, Ann. Phys. 8 (1959) 551

KL77 R. Klem, G. Igo, R. Talaga, A. Wriekat, H. Courant, K. Einsweiler, T. Joyce, H. Kagan, Y. Makidisi, M. Marshak, B. Mossberg, E. Peterson, K. Russick and T. Walsk, Phys. Rev. Lett. 38 (1977) 1272

KU70 E. Kujawski, Phys. Rev. C1 (1970) 1651

LA55 A.M. Lane and C.F. Wandel, Phys. Rev. 98 (1955) 1524

MC65 P.G. McManigal, R.D. Eandi, S.N. Kaplan and B.J. Moyer, Phys. Rev. 137 (1965) B620

PA67A H. Palevsky, J.L. Friedes, R.J. Sutter, G.W. Bennets, G.J. Igo, W.D. Simpson, G.C. Phillips, D.M. Corley, W.S. Wall. R.l. Stearns and B. Gottschalk, Phys. Rev. Lett. 18 (1967) 1200

PA67B G. Passatore, Nul. Phys. A95 (1967) 694

PA68 G. Passatore, Nul. Phys. A110 (1968) 91

PA75 G. Passatore, Nul. Phys. A248 (1975) 509

RA74 S. Ramanataram, C.L. Rad and K. Ramanataram, Nucl. Phys. A226 (1974) 173

RU75A D.W. Rule and Y. Hahn, Phys. Rev. C12 (1975) 1607

RU75B D.W. Rule and Y. Hahn, Phys. Rev. C12 (1975) 1616

RU75C D.W. Rule and Y. Hahn, Phys Lett. 34 (1975) 332

RU76 D.W. Rule and Y. Hahn, Phys. Rev. C14 (1976) 1102

SA73 A.M. Saperstein, Phys. Rev. C7 (1973) 466

SC76 The Saclay Group (privat commication).

SE65 M.A. Melkanoff, M.B. Epstein and T. Sawada, U.C.L.A. Report No.66-10 (unpublished).

SI76 I. Sick, J.S. McCarthy and R.R. Whitney, Phys. Lett. 64B (1976) 33

TA71 Y.C. Tang and R.E. Brown, Phys. Rev. C4 (1971) 1979

TH70 G.E. Thompson M.B. Epstein and T. Sawada, Nul. Phys. A142 (1970) 571

VA73 W.T.H. VanOers and Huang Haw, Phys. Lett. 45B (1973) 227

VA75 W.T.H. VanOers, Huang Haw, N.E. Davison, A. Ingemarsson, B. Fagerstron and G. Tibell, Phys. Rev. C10 (1974) 307

VE75 S.L. Verbeck, J.C, Fong, G. Igo, G.A. Whitten Jr.,

D.L. Hendrie, Y Terrien, V. Pereze - Mendez and G.W. Hoffmann, Phys. Lett. 59B (1975) 339

VO74 L.G. Votta, P.G. Roos, N.S. Chart and R. Woody III, Phys. Rev C10 (1974) 520

WA53 N.C. Francis and K.M. Watson, Phys. Rev. 92 (1952) 291

WA56 W.B. Riesenfeld and K.M. Watson, Phys. Rev. 102 (1956) 1157

WA57 K.M. Watson, Phys. Rev. 105 (1957) 1388

WA71 S.J. Wallace, Phys. Rev. Lett. 27 (1971) 622

WA77 S.J. Wallace and Y. Alexander, (private commuication).

APPENDIX

SEEK

An Optical Potential Search Program

The automatic search for best fit parameters were carried out by the computing code 'SEEK', which is a well known program written a few years ago by the U.C.L.A. Group (SE65). The Fortran program is used for carrying out Optical Model analyses of elastic scattering data of spin-0 or spin-1/2 particles scattered on complex nuclei. The program permits automatic searchs over the space of the nuclear optical model parameter space yielding optimum fits to the cross-section and polarization data.

The program employs the Schrodinger Equation to calculate the elastic scattering amplitude from which observables such as crossection, polarization and total cross-section are obtained. The Schrodingrer equation for the system is given by:

$$\left(\frac{-\hbar^2}{2\mu} \nabla^2 + V \right) \Psi = E\Psi \qquad \text{A.1}$$

where μ is the reduced mass, E is the energy in the centre of mass, and V is the scattering potential.

Due to the necessity to fit the large-angle data, the Optical Model Potential described in Eq.(A.1) has been modified to include an Exchange Potential. The modified

potential has the form

$$V = V_c(r) + V_r(r) + (-1)^{\ell} V_{ex}(r)$$

$$+ i(W_v(r) + W_s(r)) + 2[V_{s\cdot o}(r) + iW_{s\cdot o}(r)]\vec{\sigma}\cdot\vec{\ell} \qquad \text{A.2}$$

where r is the relative distance and Vc(r), Vr(r), Vex(r), Wv(r), Ws(r), Vs.o(r) and Ws.o(r) represents respectively the Coulomb, Central Real, Exchange, Central Imaginary, Surface Imaginary, Spin-orbit Real and Spin-orbit Imaginary, respectively. These terms are all assumed to be spherically symmetric. Separating the radial and angular parts Eqs. (A.1) and (A.2) give:

$$\left(\frac{d^2}{d\rho^2} - \frac{\ell(\ell+1)}{\rho^2} + 1 - \frac{V_\ell^j}{E} \right) \psi_\ell^j(r) = 0 \qquad \text{A.3}$$

where

$$V_\ell^j = V_c(r) + V_r(r) + (-1)^{\ell} V_{ex}(r) + i[W_v(r) + W_s(r)]$$

$$+ 2[V_{s\cdot o}(r) + iW_{s\cdot o}(r)] \begin{cases} \ell & \\ -\ell-1 & \end{cases} \qquad \text{A.4}$$

where $\rho = kr$. and the factor 1 correspondes to $j=1+1/2$ while -1-1 corresponds to $j=1-1/2$. At a large distance $r=r_m$ the wave function $\psi_\ell^j(r_m)$ is matched to a linear combination of regular and out going coulomb wave functions.

$$\psi_\ell^j(r_m) = F_\ell(n,kr_m) + C_\ell^j[G(n,kr_m) + iF_\ell(n,kr_m)] . \qquad \text{A.5}$$

For a spin-1/2 incident particle, the two independent scattering amplitudes are:

$$A(\Theta) = f_c(\Theta) + \frac{1}{k}\sum_{\ell=1}^{\infty} e^{2i\sigma_\ell}\,[(\ell+1)C_\ell^{\ell+1} + \ell C_\ell^{\ell-1/2}]P_\ell(\cos\Theta) \qquad A.6$$

$$B(\Theta) = \frac{-1}{k}\sum_{\ell=0}^{\infty} e^{2i\sigma_\ell}[C_\ell^{\ell+1/2} - C_\ell^{\ell-1/2}]P_\ell^1(\cos\Theta) \qquad A.7$$

where

$$f_c(\Theta) = \frac{-\eta \exp[i\eta \ln(\sin^2\Theta/2 + 2i\sigma_0)]}{2k\sin^2\Theta/2} \qquad A.8$$

The differential cross-section and the polarization for an unpolarized incident beam is given by:

$$\sigma(\Theta) = |A(\Theta)|^2 + |B(\Theta)|^2 \qquad A.9$$

$$P(\Theta) = (A^*B + B^*A)/\sigma(\Theta) \qquad A.10$$

The reaction cross-section σ_r is given by:

$$\sigma_r = \frac{4\pi}{k^2}\sum_{\ell=0}^{\infty}\{(\ell+1)[\,\mathrm{Im}C_\ell^{\ell+1/2} - |C_\ell^{\ell+1/2}|^2] + [\,\mathrm{Im}C_\ell^{\ell-1/2} - |C_\ell^{\ell-1/2}|\} \qquad A.11$$

Thus the necessary input parameters are:

Geometrical Parameters.

Rc, Rr, Ri, Rs.o, Rex, Ar, Ai, As.o, Aex.

Dynamical parameters.

V, Wv, Ws, Vs.o, Ws.o, Vex.

The program searches for a set of best fit parameters by minimizing the total χ^2 defined by:

$$\chi^2(\theta_i) = \chi^2_\sigma(\theta_i) + \chi^2_p(\theta_i) \qquad \text{A.12}$$

where

$$\chi^2_\sigma(\theta_i) = \sum_m \left|(\sigma^{th}_m(\theta_i) - \sigma^{ex}_m/\Delta\sigma^{ex}_m)\right|^2 \qquad \text{A.13}$$

and

$$\chi^2_p(\theta_i) = \sum_{m'} \left|(p^{th}_{m'}(\theta_i) - p^{ex}_{m'}/\Delta p^{ex}_{m'})\right|^2 \qquad \text{A.14}$$

The program is capable of searching on all variables simultaneously, however, this would led to large comsumption of computing time and requires a large memory space from the computer, therefore the number of search variables is limited to two at any given search.